UNIVERSIDAD DE CONCEPCIÓN

Centro de Investigación en
Ingeniería Matemática (CI^{2}MA)

A high order unfitted HDG method for the Helmholtz equation with first order absorbing boundary condition

Liliana Camargo, Manuel Solano

PREPRINT 2021-27

SERIE DE PRE-PUBLICACIONES

A high order unfitted HDG method for the Helmholtz equation with first order absorbing boundary condition

Liliana Camargo[3] and Manuel Solano[1,2]

[1]Departamento de Ingeniería Matemática, Facultad de Ciencias Físicas y Matemáticas, Universidad de Concepción, Concepción, Chile.
[2]Centro de Investigación en Ingeniería Matemática (CI^{2}MA), Universidad de Concepción, Concepción, Chile.
[3]Grupo de Investigación Computación Científica, Universidad Nacional de Colombia, sede Medellín

November 2, 2021

Abstract

This work analyzes a high order unfitted hybridizable discontinuous Galerkin (HDG) method for the Helmholtz equation in a non-polyhedral domain Ω with first order absorbing boundary condition. The HDG method is posed in a polyhedral subdomain Ω_h whose boundary is at a distance δ from the boundary of Ω. The absorbing boundary data is properly transferred from $\partial\Omega$ to $\partial\Omega_h$ in such a way that the method achieves high order accuracy. We first derive a stability analysis and then obtain the corresponding *a priori* error estimates, with the explicit dependence on the wavenumber κ, the meshsize h, the distance between the boundaries δ and the stabilization parameter of the method. Finally, the theoretical rates of convergence are supported by numerical experiments.

1 Introduction.

For a given source term $f \in L^2(\Omega)$ and a prescribed boundary data $g \in H^{1/2}(\Gamma)$, we consider the problem of seeking $(u, \boldsymbol{q})$ which satisfies the following Helmholtz equation in mixed form, defined in a non-polyhedral domain $\Omega \subset \mathbb{R}^d$ $(d = 2, 3)$ with compact Lipschitz boundary Γ:

$$\boldsymbol{q} + \nabla u = 0 \quad \text{in} \quad \Omega, \tag{1a}$$

$$\nabla \cdot \boldsymbol{q} - \kappa^2 u = f \quad \text{in} \quad \Omega, \tag{1b}$$

$$-\boldsymbol{q} \cdot \boldsymbol{n}_\Gamma + i\,\kappa u = g \quad \text{on} \quad \Gamma := \partial\Omega, \tag{1c}$$

where $\boldsymbol{n}_\Gamma$, $i = \sqrt{-1}$ and $\kappa > 0$ denote the unit outward normal vector, the imaginary unit and the wavenumber, respectively. Since we are interested in analyzing the case of a large wavenumber, without loss of generality, we consider $\kappa \geq 1$.

There is a vast literature on the characterization and approximation of the solutions of the Helmholtz problem in two or three dimensions and it is widely known that the problems with large wavenumbers have highly oscillatory solutions [1] and therefore the system of equations could be ill-conditioned or difficult to solve numerically. In particular, one of the most attractive numerical scheme is the discontinuous Galerkin (DG) method, due to its flexibility of choosing different polynomial degrees on each local approximation space and also meshes with hanging nodes. However, DG methods yield to a very large linear system to solve, which in the case of Helmholtz equations is the main drawback for high wavenumbers. With the aim to circumvent this difficulty, hybridization of DG method were proposed by [4]. Since then, a wide variety of equations have been solved numerically by using hybridizable discontinuous Galerkin (HDG) schemes. The HDG method does not present the disadvantage of nodal duplication along the inter-element boundaries since its globally coupled unknowns are single-valued numerical traces defined on the element boundaries. Moreover, it can be efficiently implemented by employing static condensation and parallelization.

The first h-version analysis of an HDG method for the Helmholtz equation was provided in [16] for a Dirichlet boundary value problem posed on a polyhedral Lipschitz domain where, considering the projection-based error analysis of HDG methods [5] and a duality argument, the authors proved optimal convergence rates for all the variables under the constraint κh sufficiently small, and constants which depend implicitly on the wavenumber. On the other hand, also considering a first order absorbing boundary condition and a star-shaped domain respect to a point, the authors in [3] proved that the HDG scheme is stable without any mesh constraint. Recently, for the linear case, [32] showed optimal error estimates under the condition $\kappa^3 h^2$ small enough. In all these HDG methods, the choice of a complex-valued stabilization parameter plays a key role in controlling the pollution error, as can be seen in the dispersion analysis performed in [15].

All the aforementioned methods are for polyhedral domains and, for that reason, the focus of our work is to deal with a high order approximation on domains having a curved boundary. In general, it is possible to distinguish in the literature two different approaches to deal with non-polygonal domains: fitted and unfitted methods. In both cases, since the boundary condition is prescribed in Γ, the challenge is determining how to impose a proper boundary data on Γ_h and preserve high order accuracy. For a complete discussion about both families of methods, we refer the reader to [9, 11, 21, 23, 22] and the references therein. Briefly speaking, in the first approach the computational boundary Γ_h somehow "fits" or resolves the original boundary Γ with certain degree of accuracy. For instance, when the solution is approximated by piecewise linear functions, Γ_h can be constructed by means of piecewise linear interpolation of Γ. For high order polynomial degree approximation, isoparametric finite element methods [20] or isogeometric analysis [18] can be used. In the second approach, the computational boundary Γ does not necessarily fit Γ, as in the immerse boundary method [24]. It is usually based on background meshes that facilitates its implementation in complex geometries. However, the main drawback of these types of methods is their low order approximation, due to the fact that Γ_h is "far" from Γ. During the last decade, several contributions have been made with the aim to combine the flexibility in the mesh construction of unfitted methods with a high order approximation. For instance, the authors in [7, 9, 11] proposed and analyzed a novel technique, which consists of transferring the boundary data from Γ to Γ_h by integrating a local extrapolation of the gradient approximation. Even though this idea does not depend on the Galerkin method employed, as long as the gradient of the solution is one of the unknowns, it has been applied mainly in the context of HDG methods [21, 25, 27, 28, 29, 30, 31] and also in mixed finite element methods [22, 23].

The main purpose of this work is to propose an HDG method for (1) posed in a curved domain Ω that is approximated by a polyhedral computational domain. The boundary condition (1c) is properly transferred to the computational boundary in such a way that the method acquires high order precision. To that end, we generalize the transferring technique in [10, 11], originally developed for Dirichlet boundary data, for the boundary condition (1c). Although the purpose of this work consists of quantifying the effect of the wavenumber on the accuracy of the approximation on the curved domain, a side consequence is that the study that we will present here also allow us to deal with a Neumann boundary data. We would like to point out that the authors in [25] proposed a way to handle Neumann boundary conditions by using a method that requires the distance between Γ_h and Γ to be of order of the square of the meshsize, but they did not include any error analysis. In this way, one of the side contribution of our work is to provide an improvement of the technique in [25] and the corresponding theoretical framework.

We provide the stability and error analysis of our scheme by considering an energy argument to deduce a Gårding type identity and a duality argument to bound the L^2-norm of the approximation of the scalar unknown. We will show that the stability of the scheme holds for a meshsize h such that $h\kappa$ is sufficiently small. The deduced error estimates allow us to affirm that the method achieves optimal convergence rates for both unknowns. In other words, we carry out a study that extends the known *a priori* error analysis for the Helmholtz equation, to the case where the domain is non-polyhedral and the boundary data is transferred through local extrapolations. We also establish, explicitly, the influence of the wavenumber and meshsize on the closeness conditions between the computational boundary Γ_h and the true boundary Γ that must be satisfied in order to ensure the stability and convergence of the method.

The remainder of the paper is organized as follows. In Section 2 we introduce notation and the concept of admissible subdomains and triangulations. Then, we present in Section 3 the unfitted HDG scheme and its stability analysis is shown in Section 4. In Section 5 we carry out the corresponding error analysis. In the last section the performance of the method is illustrated by means of numerical simulations. Finally, we end with conclusion and a discussion.

2 Notation and computational domain.

This section is devoted to recall standard notation regarding HDG methods and introduce the terminology related to the unfitted method. Even though most of the notation and definitions are nowadays somehow standard in this type of methods and they have been introduced in several works [9, 21, 26, 27], we state them here in order to make this manuscript self-contained.

Families of admissible subdomains and admissible triangulations. We say $\{\Omega_J\}_{J>0}$ is a *family of admissible subdomains* if it satisfies the following five conditions. For each $J>0$, (1) $\Omega_J \subseteq \Omega$ is simply connected, (2) $\Gamma_J := \partial\Omega_J$ is a polygon with unit normal $\boldsymbol{n}_J$ pointing outwards Ω_J and (3) there exists a bijection $\phi_J : \Gamma_J \to \Gamma$. Moreover, for every $\delta > 0$ there are infinite many indices J satisfying that (4) $\mathrm{dist}(\Gamma_J, \Gamma) \leq \delta$ and (5) $\|\boldsymbol{n}_\Gamma - \boldsymbol{n}_J \circ \phi_J^{-1}\|_{\infty,\Gamma} \leq C_\Gamma\, \delta^\alpha$, for some non-negative constants C_Γ and α. We observe that the first four conditions ensure that the family of admissible subdomains will exhaust Ω, whereas the last one establishes that the normal vectors of the subdomains uniformly aligns with the normal of Ω when δ aproaches zero. On the other hand, let us note that if the first condition is removed, the subdomains will still exhaust Ω, but we will keep it for the sake of clarity of the explanations.

Let $\{\Omega_J\}_{J>0}$ be a family of admissible subdomains and $\delta > 0$. We say that $\{\mathcal{T}_h^\delta\}_{h>0}$ is a *family of simplicial δ-admissible triangulations* if, for each $h > 0$, $\mathcal{T}_h$ satisfies the following conditions: (1) it is a triangulation for at least one admissible subdomain Ω_J, (2) it is a shape-regular tetrahedrization of Ω_J i.e., there exists $\gamma > 0$ such that for all elements $K \in \mathcal{T}_h$, $h_K/\rho_K \leq \gamma$, where h_K is the diameter of K and ρ_K is the diameter of the largest ball contained in K, (3) the meshsize $h := \max_{K\in\mathcal{T}_h} h_K$ satisfies $\delta \leq Ch$ for some non-negative constant C; and (4) for each facet e, $|e|$ is proportional to $|\phi(e)|$, where $|\cdot|$ denotes the Lebesgue measure. For the aforementioned admissible subdomain Ω_J in condition (1), we set $\Omega_{h,J}$ as the union of elements $K \in \mathcal{T}_h^\delta$, which will be referred as *computational domain.* For the sake of simplicity of notation we write Ω_h, Γ_h and $\boldsymbol{n}_{\Gamma_h}$ instead of $\Omega_{h,J}$, Γ_J and $\boldsymbol{n}_J$, respectively.

Similarly, the bijection ϕ_J will be just denoted by ϕ. From now on, we will drop the upper index δ and consider always a family of δ-admissible triangulation $\{\mathcal{T}_h\}_{h>0}$. We also set $\partial\mathcal{T}_h := \{\partial K : K \in \mathcal{T}_h\}$ and $\mathcal{E}_h := \mathcal{E}_I \cup \mathcal{E}_\Gamma$, where $\mathcal{E}_I$ and $\mathcal{E}_\Gamma$ denote the interior and boundary facets, respectively. Furthermore, h_e will represent the diameter of a given face $e \in \mathcal{E}_h$ and for every element K, we will denote by $\boldsymbol{n}_K$ the outward unit normal vector to K, writing $\boldsymbol{n}$ instead of $\boldsymbol{n}_K$ when there is no confusion.

Remark 1. *If Ω is convex, we can construct a polyhedral domain Ω_h such that its boundary Γ_h is the piecewise linear interpolation of Γ. In this case, Ω_h is an admissible subdomain with $\delta = \mathcal{O}(h^2)$ and $\alpha = 1/2$. Moreover, any simplicial triangulation of Ω_h is δ-admissible. On the other hand, this property also holds for a non-convex domain since the condition $\Omega_h \subset \Omega$ is not essential, see Remark* 3.2 *in [22].*

Spaces and norms. Given an element K and a non-negative integer k, $\mathbb{P}_k(K)$ and $\mathbb{P}_k(e)$ denote the spaces of polynomials of total degree at most k on K and on e, respectively. We also define $\mathbf{P}_k(K) := [\mathbb{P}_k(K)]^d$. On the other hand, given a region $D \subset \mathbb{R}^d$, we denote by $(\cdot,\cdot)_D$ and $\langle\cdot,\cdot\rangle_{\partial D}$ the $\mathrm{L}^2(D)$ and $\mathrm{L}^2(\partial D)$ complex inner products, respectively. The L^2-norms over D and ∂D will be denoted by $\|\cdot\|_D$ and $\|\cdot\|_{\partial D}$. We use the standard notation for Sobolev spaces and their associated norms and seminorms, where vector-valued functions and their corresponding spaces are denoted in bold face.

In addition, given a triangulation $\mathcal{T}_h$, we introduce the following finite dimensional spaces of piecewise polynomials

$$\begin{aligned}
\boldsymbol{V}_h &:= \{\boldsymbol{v} \in \mathbf{L}^2(\mathcal{T}_h) : \boldsymbol{v}|_K \in \mathbf{P}_k(K),\ \forall\ K \in \mathcal{T}_h\},\\
W_h &:= \{w \in \mathrm{L}^2(\mathcal{T}_h) : w|_K \in \mathbb{P}_k(K),\ \forall\ K \in \mathcal{T}_h\},\\
M_h &:= \{\mu \in \mathrm{L}^2(\mathcal{E}_h) : \mu|_e \in \mathbb{P}_k(e),\ \forall\ e \in \mathcal{E}_h\},
\end{aligned}$$

and the inner products $(\cdot,\cdot)_{\mathcal{T}_h} := \sum_{K\in\mathcal{T}_h} (\cdot,\cdot)_K$, $\langle\cdot,\cdot\rangle_{\partial\mathcal{T}_h} := \sum_{K\in\mathcal{T}_h} \langle\cdot,\cdot\rangle_{\partial K}$ with their corresponding norms

$$\|\cdot\|_{\Omega_h} := \left(\sum_{T\in\mathcal{T}_h} \|\cdot\|_T^2\right)^{1/2}, \qquad \|\cdot\|_{\partial\mathcal{T}_h} := \left(\sum_{T\in\mathcal{T}_h} \|\cdot\|_{\partial T}^2\right)^{1/2} \quad \text{and} \quad \|\cdot\|_{\Gamma_h} := \left(\sum_{e\in\mathcal{E}_\Gamma} \|\cdot\|_e^2\right)^{1/2}.$$

Transferring paths and extension patch. Let us consider the mapping $\boldsymbol{\phi} : \Gamma_h \to \Gamma$ and, for each point $\boldsymbol{x} \in \Gamma_h$, we write $\overline{\boldsymbol{x}} = \boldsymbol{\phi}(\boldsymbol{x}) \in \Gamma$. We denote by $\sigma(\boldsymbol{x})$ the segment starting at $\boldsymbol{x}$ and ending at $\overline{\boldsymbol{x}}$, with unit tangent vector $\boldsymbol{t}(\boldsymbol{x})$ and length $l(\boldsymbol{x}) := |\sigma(\boldsymbol{x})|$. The segment $\sigma(\boldsymbol{x})$ is referred as the *transferring paths* associated to $\boldsymbol{x}$ and it is assumed to satisfy two conditions: it does not intersect the interior of another segment and its length $|\sigma(\boldsymbol{x})|$ is of order at most δ.

For $e \in \mathcal{E}_\Gamma$, we define the *extension patch* as

$$K_{ext}^e := \{\boldsymbol{x} + s\boldsymbol{t}(\boldsymbol{x}) : 0 \le s \le l(\boldsymbol{x}), \boldsymbol{x} \in e\}.$$

Since the HDG solution will be computed in the computational domain Ω_h, this extension patch will be used to "extend" the solution to the entire domain Ω.

Now, for a smooth enough $\boldsymbol{p}$, let us introduce the norm $|||\cdot|||_e$,

$$|||\boldsymbol{p}|||_e := \left(\int_e \int_0^{l(\boldsymbol{x})} |\boldsymbol{p}(\boldsymbol{x} + s\boldsymbol{t}(\boldsymbol{x}))|^2 \, ds \, dS_{\boldsymbol{x}}\right)^{1/2}, \tag{2}$$

which, under certain conditions, is equivalent to the $\mathrm{L}^2(K^e_{ext})$-norm. For instance, in two dimensions, let $\boldsymbol{u}$ and $\boldsymbol{v}$ be the vertices of the edge e, and for $\boldsymbol{w} \in \{\boldsymbol{u}, \boldsymbol{v}\}$, we set $\boldsymbol{m}^{\boldsymbol{w}} := \boldsymbol{t}(\boldsymbol{w})/|\boldsymbol{t}(\boldsymbol{w})|$ if $\boldsymbol{t}(\boldsymbol{w}) \neq \mathbf{0}$ and $\boldsymbol{m}^{\boldsymbol{w}} := \boldsymbol{n}_e$, otherwise. Therefore, a point $\boldsymbol{x}$ on e can be represented as $\boldsymbol{x}(\theta) = \boldsymbol{u}+\theta(\boldsymbol{v}-\boldsymbol{u})$ for $\theta \in [0,1]$ and the tangent vector of the path associated to $\boldsymbol{x}$ can be written as $\widehat{\boldsymbol{m}}(\theta) := \boldsymbol{m}^{\boldsymbol{u}} + \theta(\boldsymbol{m}^{\boldsymbol{v}} - \boldsymbol{m}^{\boldsymbol{u}})$. Moreover, the normalized tangent vector can be written as $\boldsymbol{m}(\theta) := \widehat{\boldsymbol{m}}(\theta)/|\widehat{\boldsymbol{m}}(\theta)|$ if $\widehat{\boldsymbol{m}}(\theta) \neq \mathbf{0}$; and $\boldsymbol{m}(\theta) = \boldsymbol{n}_e$, otherwise. We recall Lemma 3.4 in [22]:

Lemma 2. *Let $\boldsymbol{p} \in \mathrm{L}^2(K^e_{ext})$. In addition, let us consider the following conditions:*

(i) $\boldsymbol{m}^{\boldsymbol{u}} \cdot \boldsymbol{p}^{\boldsymbol{v}} \geq 0$,

(ii) there exists constant β_e, independent of h, such that $\boldsymbol{m}(\theta) \cdot \boldsymbol{n}_e \geq \beta_e > 0$ for all $\theta \in [0,1]$; and

(iii) $\boldsymbol{m}^{\boldsymbol{u}} \cdot (\boldsymbol{m}^{\boldsymbol{v}})^{\perp} \geq 0$.

If (i) holds, then there exists $C^e_2 > 0$ such that

$$\|\boldsymbol{p}\|_{K^e_{ext}} \leq C^e_2 |||\boldsymbol{p}|||_e. \tag{3}$$

Moreover, if (ii) and (iii) hold, then there exists $C^e_1 > 0$ such that

$$C^e_1 |||\boldsymbol{p}|||_e \leq \|\boldsymbol{p}\|_{K^e_{ext}}. \tag{4}$$

We point out that, if $\boldsymbol{m}^{\boldsymbol{u}}$ is parallel to $\boldsymbol{m}^{\boldsymbol{v}}$, then $|||\boldsymbol{p}|||_e = \|\boldsymbol{p}\|_{K^e_{ext}}$ and conditions (i)-(iii) are not required. In three dimensions a similar result holds, according to Lemma A.1 in [23].

Extrapolation operator. The region enclosed by Ω and Ω_h will be denoted by Ω^c_h. Since Ω^c_h is not meshed, the HDG approximation of the flux $\boldsymbol{q}$ will be locally extrapolated, on each extension patch, from the computational domain Ω_h to Ω^c_h. More precisely, let $e \in \mathcal{E}_\Gamma$ and the element K_e where e belongs. Let $\boldsymbol{p}|_{K_e} : \mathbf{P}_k(K_e) \to \mathbb{R}$ be a vector-valued polynomial function. We will define its extrapolation to K^e_{ext} as

$$\boldsymbol{E}_h(\boldsymbol{p})(\boldsymbol{y})|_{K^e_{ext}} := \boldsymbol{p}|_{K_e}(\boldsymbol{y}) \qquad \forall\, \boldsymbol{y} \in K^e_{ext}. \tag{5}$$

Note that the extended function $\boldsymbol{E}_h(\boldsymbol{p})(\boldsymbol{y})|_{K^e_{ext}}$ is a vector-valued polynomial function whose support includes Ω^c_h. Each element K will have its own extended function. If there is no confusion, we just write $\boldsymbol{v}_h$ instead of $\boldsymbol{E}_{\boldsymbol{h}}(\boldsymbol{v}_h)$.

On the other hand, we will denote by $h^{\perp}_e$ (resp. δ_e) the largest distance between a point of K_e (resp. K^e_{ext}) and the plane determined by the facet e. We define

$$C^e_{ext} := (\delta_e)^{-1/2}(h^{\perp}_e)^{1/2} \sup_{\substack{\boldsymbol{v}_h \in \mathbf{P}_k(K_e) \\ \boldsymbol{v}_h \neq \mathbf{0}}} \frac{|||\boldsymbol{v}_h|||_e}{\|\boldsymbol{v}_h\|_{0,K_e}}, \tag{6}$$

where, the constant C^e_{ext} is independent of the meshsize h, but depends on the shape-regularity constant γ and on the polynomial degree; see Appendix in [22]. Finally, we note that $\delta \geq \max_{e \in \mathcal{E}_\Gamma} \delta_e$.

3 The numerical method.

3.1 The equations in Ω_h.

We consider a computational domain Ω_h and a δ-admissible triangulation $\mathcal{T}_h$. Then, by restricting (1) to Ω_h, we write

$$\boldsymbol{q} + \nabla u = 0 \quad \text{in} \quad \Omega_h, \tag{7a}$$

$$\nabla \cdot \boldsymbol{q} - \kappa^2 u = f \quad \text{in} \quad \Omega_h, \tag{7b}$$

$$-\boldsymbol{q} \cdot \boldsymbol{n}_{\Gamma_h} + i\,\kappa u = \varphi \quad \text{on} \quad \Gamma_h := \partial\Omega_h, \tag{7c}$$

where φ is a boundary data that we need to specify and $\boldsymbol{n}_{\Gamma_h}$ is the unit outward normal vector of the domain Ω_h. In the context of pure diffusion problems, a way to determine φ was proposed for one dimension in [7] and then extended to higher dimensions by [11]. The method consists of transferring the data from Γ to Γ_h along the transferring paths. Let $\boldsymbol{x} \in \Gamma_h$ and $\overline{\boldsymbol{x}} := \phi(\boldsymbol{x}) \in \Gamma$. After integrating (1a) along the segment connecting $\boldsymbol{x}$ and $\overline{\boldsymbol{x}}$, we have

$$u(\boldsymbol{x}) = u(\overline{\boldsymbol{x}}) + \int_0^{l(\boldsymbol{x})} \boldsymbol{q}(\boldsymbol{x} + \boldsymbol{t}(\boldsymbol{x})s) \cdot \boldsymbol{t}(\boldsymbol{x})\,\mathrm{d}s,$$

which, according with (1c), is equivalent to

$$i\,\kappa u(\boldsymbol{x}) = \boldsymbol{q} \cdot \boldsymbol{n}_\Gamma(\overline{\boldsymbol{x}}) + g(\overline{\boldsymbol{x}}) + i\,\kappa \int_0^{l(\boldsymbol{x})} \boldsymbol{q}(\boldsymbol{x} + \boldsymbol{t}(\boldsymbol{x})s) \cdot \boldsymbol{t}(\boldsymbol{x})\,ds. \tag{8}$$

Finally, arranging terms based on φ given in (7c), we obtain

$$\varphi(\boldsymbol{x}) = \boldsymbol{q} \cdot \boldsymbol{n}_\Gamma(\overline{\boldsymbol{x}}) - \boldsymbol{q} \cdot \boldsymbol{n}_{\Gamma_h}(\boldsymbol{x}) + g(\overline{\boldsymbol{x}}) + i\,\kappa \int_0^{l(\boldsymbol{x})} \boldsymbol{q}(\boldsymbol{x} + \boldsymbol{t}(\boldsymbol{x})s) \cdot \boldsymbol{t}(\boldsymbol{x})\,ds. \tag{9}$$

In other words, we have obtained an identity that relates the Robin boundary data φ on Γ_h with the gradient of the solution $\boldsymbol{q}$ and the data g on Γ.

3.2 The HDG method.

The HDG scheme associated to (7) seeks $(\boldsymbol{q}_h, u_h, \widehat{u}_h) \in \boldsymbol{V}_h \times W_h \times M_h$, an approximation of $(\boldsymbol{q}, u, u|_{\mathcal{E}_h})$ in Ω_h, such that

$$(\boldsymbol{q}_h, \boldsymbol{v})_{\mathcal{T}_h} - (u_h, \nabla \cdot \boldsymbol{v})_{\mathcal{T}_h} + \langle \widehat{u}_h, \boldsymbol{v} \cdot \boldsymbol{n} \rangle_{\partial\mathcal{T}_h} = 0, \tag{10a}$$

$$-(\boldsymbol{q}_h, \nabla w)_{\mathcal{T}_h} + \langle \widehat{\boldsymbol{q}}_h \cdot \boldsymbol{n}, w \rangle_{\partial\mathcal{T}_h} - \kappa^2 (u_h, w_h)_{\mathcal{T}_h} = (f, w)_{\mathcal{T}_h}, \tag{10b}$$

$$\langle \widehat{\boldsymbol{q}}_h \cdot \boldsymbol{n}, \mu \rangle_{\partial\mathcal{T}_h \setminus \Gamma_h} = 0, \tag{10c}$$

$$\langle -\widehat{\boldsymbol{q}}_h \cdot \boldsymbol{n}_{\Gamma_h} + i\kappa \widehat{u}_h, \mu \rangle_{\Gamma_h} = \langle \varphi_h, \mu \rangle_{\Gamma_h}, \tag{10d}$$

for all $(\boldsymbol{v}, w, \mu) \in \boldsymbol{V}_h \times W_h \times M_h$. Here,

$$\widehat{\boldsymbol{q}}_h \cdot \boldsymbol{n} := \boldsymbol{q}_h \cdot \boldsymbol{n} + i\tau(u_h - \widehat{u}_h) \quad \text{on} \quad \partial\mathcal{T}_h, \tag{10e}$$

for τ being a positive stabilization function such that $\tau_{min} := \min_{e \in \mathcal{E}_h} \tau_e$ and $\tau_{max} := \max_{e \in \mathcal{E}_h} \tau_e$. Furthermore, the approximate boundary condition motivated by (9), is given by

$$\varphi_h(\boldsymbol{x}) = \boldsymbol{q}_h \cdot \boldsymbol{n}_\Gamma(\overline{\boldsymbol{x}}) - \boldsymbol{q}_h \cdot \boldsymbol{n}_{\Gamma_h}(\boldsymbol{x}) + g(\overline{\boldsymbol{x}}) + i\,\kappa \int_0^{l(\boldsymbol{x})} \boldsymbol{q}_h(\boldsymbol{x} + \boldsymbol{t}(\boldsymbol{x})s) \cdot \boldsymbol{t}(\boldsymbol{x})\,ds, \tag{10f}$$

where we point out that $\boldsymbol{q}_h$ is being evaluated outside of the computational domain Ω_h and is understood as the extrapolation defined in (5).

3.3 Reconstruction on Ω_h^c.

The HDG scheme (10) provides an approximation of the solution in the computational domain Ω_h. With the aim to complete the approximation of $\boldsymbol{q}$ and u in Ω, in this section we will explain how an approximation in Ω_h^c can be calculated.

First of all, for the approximation of $\boldsymbol{q}$ outside Ω_h, we use the extrapolation operator defined in (5).

On the other hand, based on (8) we propose the following approximation of u in Ω_h^c. For any point $\boldsymbol{y} \in K_{ext}^e$, there is a transferring paths $\sigma(\boldsymbol{x})$ starting at $\boldsymbol{x} \in \Gamma_h$ and ending at $\overline{\boldsymbol{x}} = \phi(\boldsymbol{x}) \in \Gamma$, so that we can write $\boldsymbol{y} = \boldsymbol{x} + (\eta/l(\boldsymbol{x}))(\overline{\boldsymbol{x}} - \boldsymbol{x})$ for some $\eta \in [0, l(\boldsymbol{x})]$. Then, we set

$$u_h(\boldsymbol{y}) := -i\kappa^{-1} \left(\boldsymbol{q}_h \cdot \boldsymbol{n}_\Gamma(\overline{\boldsymbol{y}}) + g(\overline{\boldsymbol{y}}) \right) + \int_0^{|\overline{\boldsymbol{y}}-\boldsymbol{y}|} \boldsymbol{q}_h(\boldsymbol{y} + \boldsymbol{t}(\boldsymbol{y})s) \cdot \boldsymbol{t}(\boldsymbol{y}) \, ds, \tag{11}$$

with $\overline{\boldsymbol{y}} := \overline{\boldsymbol{x}}$ and $\boldsymbol{t}(\boldsymbol{y}) := (\overline{\boldsymbol{y}} - \boldsymbol{y})/|\overline{\boldsymbol{y}} - \boldsymbol{y}|$.

4 Stability analysis.

In this section we provide a stability analysis by employing an energy argument to deduce first a Gårding type identity and then we derive a bound for the L^2-norm of the scalar approximation, based on a duality argument. We begin by introducing preliminary results that will be used through the analysis. With these tools at our disposal, we will move forward to the main results of this work, namely, the aforementioned stability analysis and the *a priori* error analysis. To that end, and in order to employ the stability estimates to prove well-posedness and also to deduce the error bounds, we generalize the right hand sides in (10a) and (10d), by adding the sources $\boldsymbol{G} \in \mathbf{L}^2(\Omega_h)$ and $G_\partial \in \mathrm{L}^2(\Gamma_h)$, as follows:

$$(\boldsymbol{q}_h, \boldsymbol{v})_{\mathcal{T}_h} - (u_h, \nabla \cdot \boldsymbol{v})_{\mathcal{T}_h} + \langle \widehat{u}_h, \boldsymbol{v} \cdot \boldsymbol{n} \rangle_{\partial \mathcal{T}_h} = (\boldsymbol{G}, \boldsymbol{v})_{\mathcal{T}_h}, \tag{12a}$$

and

$$\langle -\widehat{\boldsymbol{q}}_h \cdot \boldsymbol{n} + i\kappa \widehat{u}_h, \mu \rangle_{\Gamma_h} = \langle \varphi_h, \mu \rangle_{\Gamma_h} + \langle G_\partial, \mu \rangle_{\Gamma_h}. \tag{12b}$$

Since $\boldsymbol{G}$ is equal to zero in the original equation (10a) and will be equal to the error of the projection in Section 5, we consider $\boldsymbol{G}$ to be orthogonal to piecewise polynomials of degree $k-1$.

4.1 Preliminaries.

Projectors. First, let us characterize a projector commonly used in the analysis of HDG methods for elliptic problems (cf. [6, 8]),

$$\begin{aligned} \Pi_h : \boldsymbol{H}(\mathbf{div}, \mathcal{T}_h) \times H^1(\mathcal{T}_h) &\to \boldsymbol{V}_h \times W_h \\ (\boldsymbol{v}, u) &\mapsto \Pi_h(\boldsymbol{v}, u) := (\Pi_{\boldsymbol{V}} \boldsymbol{v}, \Pi_W u), \end{aligned}$$

which, for a given $K \in \mathcal{T}_h$ and a non-negative stabilization parameter τ, uniquely solves

$$\begin{aligned} (\Pi_{\boldsymbol{V}} \boldsymbol{v}, \boldsymbol{z})_K &= (\boldsymbol{v}, \boldsymbol{z})_K, && \forall \boldsymbol{z} \in \mathbf{P}_{k-1}(K) \\ (\Pi_W u, w)_K &= (u, w)_K, && \forall w \in \mathbb{P}_{k-1}(K) \\ \langle \Pi_{\boldsymbol{V}} \boldsymbol{v} \cdot \boldsymbol{n}_{\Gamma_h} + i\tau \, \Pi_W u, \mu \rangle_e &= \langle \boldsymbol{v} \cdot \boldsymbol{n}_{\Gamma_h} + i\tau \, u, \mu \rangle_e, && \forall \mu \in \mathbb{P}_k(e) \, \forall e \subset \partial K. \end{aligned} \tag{13}$$

Moreover, since we are working with complex-valued functions, it is convenient to define the following projection operator,

$$\begin{aligned}\Pi_h^* : \boldsymbol{H}(\mathbf{div}, \mathcal{T}_h) \times H^1(\mathcal{T}_h) &\to \boldsymbol{V}_h \times W_h \\ (\boldsymbol{v}, u) &\mapsto \Pi_h^*(\boldsymbol{v}, u) := (\Pi_{\boldsymbol{V}}^* \boldsymbol{v}, \Pi_W^* u),\end{aligned}$$

which, for a given $K \in \mathcal{T}_h$ and a non-negative stabilization parameter τ, uniquely solves

$$\begin{aligned}(\Pi_{\boldsymbol{V}}^* \boldsymbol{v}, \boldsymbol{z})_K &= (\boldsymbol{v}, \boldsymbol{z})_K, & \forall \boldsymbol{z} \in \mathbf{P}_{k-1}(K)\\ (\Pi_W^* u, w)_K &= (u, w)_K, & \forall w \in \mathbb{P}_{k-1}(K)\\ \langle \Pi_{\boldsymbol{V}}^* \boldsymbol{v} \cdot \boldsymbol{n}_{\Gamma_h} - i\tau\, \Pi_W^* u, \mu\rangle_e &= \langle \boldsymbol{v} \cdot \boldsymbol{n}_{\Gamma_h} - i\tau\, u, \mu\rangle_e, & \forall \mu \in \mathbb{P}_k(e)\, \forall e \subset \partial K.\end{aligned} \tag{14}$$

This additional projector will be useful during the developing of the duality argument that will lead us to obtain a stability estimate for the scalar unknown, as it will be seen in Section 4.3.

Furthermore, if $(\boldsymbol{v}, u) \in \boldsymbol{H}^{l_{\boldsymbol{v}}+1}(K) \times H^{l_u+1}(K)$, with $l_{\boldsymbol{v}}, l_u \in [0, k]$, it holds

$$\|\Pi_{\boldsymbol{V}} \boldsymbol{v} - \boldsymbol{v}\|_K \lesssim h_K^{l_{\boldsymbol{v}}+1} |\boldsymbol{v}|_{l_{\boldsymbol{v}}+1,K} + h_K^{l_u+1}\, \tau |u|_{l_u+1,K}, \tag{15a}$$

$$\|\Pi_W u - u\|_K \lesssim h_K^{l_u+1} |u|_{l_u+1,K} + h_K^{l_{\boldsymbol{v}}+1} \tau^{-1}\, |\nabla \cdot \boldsymbol{v}|_{l_{\boldsymbol{v}},K}. \tag{15b}$$

We highlight that the approximation properties (15) are also satisfied by $(\Pi_{\boldsymbol{V}}^* \boldsymbol{v}, \Pi_W^* u)$. In addition, we will use the L^2-projection $P_{M_h} : \mathrm{L}^2(\mathcal{E}_h) \to M_h$ and recall its approximation property:

$$\|P_{M_h} \rho - \rho\|_e \lesssim h_e^{l_\rho+1/2}\, |\rho|_{l_\rho+1,K},$$

for all $\rho \in H^{l_\rho+1}(K)$ with $l_\rho \in [0, k]$.

Here, we have made use of the notation $A \lesssim B$ to indicate that there exists a constant $C > 0$, independent of the meshsize and wavenumber, such that $A \le CB$. From now on, C will denote a positive constant independent of h and κ, which might take different values along the manuscript.

On the other hand, in order to obtain the error estimates on Ω_h^c, we also need the approximation properties of the extrapolation of the HDG projectors in the following lemma.

Lemma 3. *Let $\boldsymbol{v} \in \boldsymbol{H}^{m+1}(\Omega)$. There holds,*

$$\|\boldsymbol{v} - \boldsymbol{\Pi_V v}\|_{\Omega_h^c} \lesssim (1 + \delta^{1/2} h^{-1/2}) h^{m+1} \|\boldsymbol{v}\|_{\boldsymbol{H}^{m+1}(\Omega)} + \delta^{1/2} h^{-1/2} \|\boldsymbol{v} - \boldsymbol{\Pi_V v}\|_{\Omega_h} \tag{16a}$$

and

$$\|\nabla(\boldsymbol{v} - \boldsymbol{\Pi_V v})\|_{\Omega_h^c} \lesssim (1 + \delta^{1/2} h^{-1/2}) h^{m} \|\boldsymbol{v}\|_{\boldsymbol{H}^{m+1}(\Omega)} + \delta^{1/2} h^{-3/2} \|\boldsymbol{v} - \boldsymbol{\Pi_V v}\|_{\Omega_h}. \tag{16b}$$

Proof. To deduce the estimates we follow the same steps as in the proof of Lemma 3.8 of [9], but adapted to our context. Specifically, in our case we employ the norm $|\!|\!|\cdot|\!|\!|_e$ and keep track the dependence on δ.

Let us first introduce the extension operator $\boldsymbol{E} : \boldsymbol{H}^{m+1}(\Omega) \to \boldsymbol{H}^{m+1}(\mathbb{R}^d)$, for all $m \in \mathbb{Z}_0^+$, such that $\boldsymbol{E}(\boldsymbol{\rho})|_\Omega = \boldsymbol{\rho}$, for all $\boldsymbol{\rho} \in \boldsymbol{H}^{m+1}(\Omega)$ and

$$\|\boldsymbol{E}(\boldsymbol{\rho})\|_{\boldsymbol{H}^{m+1}(\mathbb{R}^d)} \lesssim \|\boldsymbol{\rho}\|_{\boldsymbol{H}^{m+1}(\Omega)}. \tag{17}$$

Then, for a given $e \in \mathcal{E}_\Gamma$, we define B_e as the ball with center $\boldsymbol{x}^{B_e}$ in the middle point of e, such that $K_{ext}^e \cup K_e \subset B_e$. We denote by $\boldsymbol{T}_e^m(\boldsymbol{E}(\boldsymbol{\rho}))$ the Taylor polynomial of degree m of the function $\boldsymbol{E}(\boldsymbol{\rho})$

around $\boldsymbol{x}^{B_e}$. Let $\boldsymbol{v} \in \boldsymbol{H}^{m+1}(\Omega)$ and denote $\boldsymbol{I}^{\boldsymbol{v}} := \boldsymbol{v} - \Pi_{\boldsymbol{V}} \boldsymbol{v}$. Then, by using the triangule inequality, (3) and (6), we have

$$\|\boldsymbol{I}^{\boldsymbol{v}}\|_{K^e_{ext}} \leq \|\boldsymbol{v} - \boldsymbol{T}^m_e(\boldsymbol{E}(\boldsymbol{v}))\|_{K^e_{ext}} + C^e_2 C^e_{ext} \delta_e^{1/2} (h^\perp_e)^{-1/2} \|\boldsymbol{T}^m_e(\boldsymbol{E}(\boldsymbol{v})) - \Pi_{\boldsymbol{V}} \boldsymbol{v}\|_{K_e},$$

from which, after adding and subtracting $\boldsymbol{v}$ in the second term and making use of the approximation properties of the Taylor polynomial ([2], Section 4.1), we obtain

$$\begin{aligned}
\|\boldsymbol{I}^{\boldsymbol{v}}\|_{K^e_{ext}} &\leq (1 + (C^e_1)^{-1} C^e_2 C^e_{ext} \delta_e^{1/2} (h^\perp_e)^{-1/2}) \|\boldsymbol{v} - \boldsymbol{T}^m_e(\boldsymbol{E}(\boldsymbol{v}))\|_{K^e_{ext}} + C^e_2 C^e_{ext} \delta_e^{1/2} (h^\perp_e)^{-1/2} \|\boldsymbol{I}^{\boldsymbol{v}}\|_{K_e} \\
&\leq (1 + (C^e_1)^{-1} C^e_2 C^e_{ext} \delta_e^{1/2} (h^\perp_e)^{-1/2}) \|\boldsymbol{E}(\boldsymbol{v}) - \boldsymbol{T}^m_e(\boldsymbol{E}(\boldsymbol{v}))\|_{B_e} + C^e_2 C^e_{ext} \delta_e^{1/2} (h^\perp_e)^{-1/2} \|\boldsymbol{I}^{\boldsymbol{v}}\|_{K_e} \\
&\lesssim (1 + (C^e_1)^{-1} C^e_2 C^e_{ext} \delta_e^{1/2} (h^\perp_e)^{-1/2}) h^{m+1} |\boldsymbol{E}(\boldsymbol{v})|_{\boldsymbol{H}^{m+1}(B_e)} + C^e_2 C^e_{ext} \delta_e^{1/2} (h^\perp_e)^{-1/2} \|\boldsymbol{I}^{\boldsymbol{v}}\|_{K_e}.
\end{aligned}$$

The result follows by (17), recalling that $h_e \lesssim h^\perp_e$ and summing over all $e \in \mathcal{E}_\Gamma$.

On the other hand, by similar arguments and employing the inverse inequality, we conclude that

$$\|\nabla(\boldsymbol{v} - \boldsymbol{\Pi_V v})\|_{K^e_{ext}} \lesssim \|\nabla \boldsymbol{v} - \nabla \boldsymbol{T}^m_e(\boldsymbol{E}(\boldsymbol{v}))\|_{K^e_{ext}} + C^e_2 C^e_{ext} \delta_e^{1/2} (h^\perp_e)^{-1/2} h^{-1}_{K_e} \|\boldsymbol{T}^m_e(\boldsymbol{E}(\boldsymbol{v})) - \Pi_{\boldsymbol{V}} \boldsymbol{v}\|_{K_e}.$$

Even more, by the approximation properties of the Taylor polynomial and (17),

$$\begin{aligned}
\|\nabla(\boldsymbol{v} - \boldsymbol{\Pi_V v})\|_{K^e_{ext}} \lesssim & h^m |\boldsymbol{E}(\boldsymbol{v})|_{\boldsymbol{H}^{m+1}(B_e)} + C^e_2 C^e_{ext} \delta_e^{1/2} (h^\perp_e)^{-3/2} \|\boldsymbol{T}^m_e(\boldsymbol{E}(\boldsymbol{v})) - \boldsymbol{v}\|_{K_e} \\
& + C^e_2 C^e_{ext} \delta_e^{1/2} (h^\perp_e)^{-3/2} \|\boldsymbol{I}^{\boldsymbol{v}}\|_{K_e} \\
\lesssim & h^m |\boldsymbol{E}(\boldsymbol{v})|_{\boldsymbol{H}^{m+1}(B_e)} + C^e_2 C^e_{ext} \delta_e^{1/2} (h^\perp_e)^{-3/2} \|\boldsymbol{T}^m_e(\boldsymbol{E}(\boldsymbol{v})) - \boldsymbol{E}(\boldsymbol{v})\|_{B_e} \\
& + C^e_2 C^e_{ext} \delta_e^{1/2} (h^\perp_e)^{-3/2} \|\boldsymbol{I}^{\boldsymbol{v}}\|_{K_e},
\end{aligned}$$

which implies (16b). $\square$

Discrete trace inequality on an extension patch. In the following result, we establish a relation between the norms $\|\cdot\|_{\Gamma_e}$ and $\|\cdot\|_{K^e_{ext}}$, for functions defined in the extension patch associated to e.

Lemma 4. *If K^e_{ext} is the corresponding extension patch of e and $\Gamma_e = \phi(e)$, then there exist positive constants $C^{tr}_{\Gamma_e}$ and C_{Γ_e}, independent of the meshsize, such that*

$$\delta_e^{1/2} \|p\|_{\Gamma_e} \leq C^{tr}_{\Gamma_e} \|p\|_{K^e_{ext}} \qquad \forall p \in \mathbb{P}_k(K^e_{ext}) \tag{18}$$

and

$$\delta_e^{1/2} \|v\|_{\Gamma_e} \leq C_{\Gamma_e} \left(\|v\|^2_{K^e_{ext}} + \delta_e \|\nabla v\|^2_{K^e_{ext}} \right)^{1/2} \qquad \forall v \in H^1(K^e_{ext}). \tag{19}$$

Proof. Let us assume $\delta_e > 0$. If not, both inequalities trivially hold true. Proceeding by a scaling argument, we define $\widehat{K^e_{ext}} := \{\widehat{\boldsymbol{y}} : \widehat{\boldsymbol{y}} = \boldsymbol{y}/\delta_e, \boldsymbol{y} \in K^e_{ext}\}$, $\widehat{p}(\widehat{\boldsymbol{y}}) := p(\boldsymbol{y}/\delta_e)$ and $\widehat{\Gamma}_e$ the part of the boundary of $\widehat{K^e_{ext}}$ that has been mapped from Γ_e. By the trace inequality in the reference patch $\widehat{K^e_{ext}}$, we have, for all $p \in \mathbb{P}_k(K^e_{ext})$, that

$$\|p\|^2_{\Gamma_e} \lesssim |\Gamma_e| \, \|\widehat{p}\|^2_{\widehat{\Gamma}_e} \lesssim |\Gamma_e| \, \|\widehat{p}\|^2_{\widehat{K^e_{ext}}} \lesssim |\Gamma_e| \, |K^e_{ext}|^{-1} \, \|p\|^2_{K^e_{ext}}.$$

The result in (18) follows by noticing that $|\Gamma_e| \delta_e$ is proportional to $|K^e_{ext}|$. The second inequality is obtained by a similar argument, but using the continuous trace inequality on the reference element. $\square$

Estimates on extrapolated functions. The following estimates will be helpful when we employ a duality argument in the forthcoming analysis (cf. Section 4.3).

Lemma 5. *If $\psi \in H^2(\Omega)$ and $\boldsymbol{\varphi} := -\nabla\psi$, it holds*

$$\|l^{-1/2}(\psi - \psi\circ\boldsymbol{\phi}) + l^{1/2}(\boldsymbol{\varphi}\circ\boldsymbol{\phi})\cdot\boldsymbol{n}\|_{\Gamma_h} \lesssim \delta\ \|\psi\|_{H^2(\Omega)},$$
$$\|l^{-1/2}(\psi - \psi\circ\boldsymbol{\phi})\|_{\Gamma_h} \lesssim \delta^{1/2}\ \|\psi\|_{H^2(\Omega)}.$$

If $\boldsymbol{\varphi} \in \boldsymbol{H}^1(\Omega)$, then

$$\|l^{-1/2}(\boldsymbol{\varphi} - \boldsymbol{\varphi}\circ\boldsymbol{\phi})\cdot\boldsymbol{n}\|_{\Gamma_h} \lesssim |\boldsymbol{\varphi}|_{\boldsymbol{H}^1(\Omega)}.$$

Let $e \in \mathcal{E}_\Gamma$, $\Gamma_e = \boldsymbol{\phi}(e)$ and K_e the element where e belongs. If $p \in \mathbb{P}_k(K_e)$, then

$$\|p - p\circ\boldsymbol{\phi}\|_e \lesssim C^e_{ext}\,\delta_e\ h_e^{-3/2}\,\|p\|_{K_e}.$$

Proof. The result follows by adapting the arguments in the proof of Lemma 1 of [21] to our context. □

4.2 Energy estimate.

We begin by showing the following Gårding-type identity.

Lemma 6. *The solution of (10), $(\boldsymbol{q}_h, u_h, \widehat{u}_h) \in \boldsymbol{V}_h \times W_h \times M_h$, satisfies*

$$\|\boldsymbol{q}_h\|^2_{\mathcal{T}_h} - \kappa^2\|u_h\|^2_{\mathcal{T}_h} - i\|\tau^{1/2}(u_h - \widehat{u}_h)\|^2_{\partial\mathcal{T}_h} - i\,\kappa\|\widehat{u}_h\|^2_{\Gamma_h} = \langle\widehat{u}_h, \varphi_h + G_\partial\rangle_{\Gamma_h} + (\boldsymbol{G}, \boldsymbol{q}_h)_{\mathcal{T}_h} + (u_h, f)_{\mathcal{T}_h}. \tag{20}$$

Proof. After defining $\boldsymbol{v} := \boldsymbol{q}_h$ in (12a), $w := u_h$ in the conjugate of (10b), integrating by parts and adding the resulting expressions, we obtain

$$\|\boldsymbol{q}_h\|^2_{\mathcal{T}_h} - \kappa^2\|u_h\|^2_{\mathcal{T}_h} + \langle u_h - \widehat{u}_h, \widehat{\boldsymbol{q}}_h\cdot\boldsymbol{n} - \boldsymbol{q}_h\cdot\boldsymbol{n}\rangle_{\partial\mathcal{T}_h} + \langle\widehat{u}_h, \widehat{\boldsymbol{q}}_h\cdot\boldsymbol{n}\rangle_{\partial\mathcal{T}_h} = (G, \boldsymbol{q}_h)_{\mathcal{T}_h} + (u_h, f)_{\mathcal{T}_h}. \tag{21}$$

Taking into account (12b), we deduce that

$$\langle\widehat{u}_h, \widehat{\boldsymbol{q}}_h\cdot\boldsymbol{n}\rangle_{\partial\mathcal{T}_h} = \langle\widehat{u}_h, \widehat{\boldsymbol{q}}_h\cdot\boldsymbol{n}\rangle_{\Gamma_h} = -\langle\widehat{u}_h, \varphi_h + G_\partial\rangle_{\Gamma_h} - i\,\kappa\|\widehat{u}_h\|^2_{\Gamma_h}.$$

Then, by substituting the above expression in (21) and using (10e), (20) follows. □

In the right hand side of (20) we observe not only the presence of the unknowns $\boldsymbol{q}_h$, u_h and $\widehat{u}_h$, but also on the transferred boundary data φ_h. The former can be treated by using the Cauchy-Schwarz inequality and the information on the left hand side(20), whereas for the latter we need the following result.

Lemma 7. *Let $e \in \mathcal{E}_\Gamma$. There holds,*

$$\|\varphi_h\|^2_e \leq \frac{1}{3}\left(C_{\delta,\kappa,h}\|\boldsymbol{q}_h\|^2_{K_e} + \|g\|^2_{\Gamma_e}\right), \tag{22}$$

where

$$C_{\delta,\kappa,h} := \max_{e\in\mathcal{E}_\Gamma}\left((C^e_{ext})^2\delta_e^2 h_e^{-3}\left(\frac{1}{2} + \kappa^2\gamma h_e^2\right) + \frac{1}{2}(C^e_2 C^{tr}_{\Gamma_e} C^e_{ext} C_\Gamma)^2\gamma\, h_e^{-1}\delta_e^{2\alpha}\right). \tag{23}$$

Proof. Let us note that, from (10f),

$$|\varphi_h(\boldsymbol{x})| \leq |\boldsymbol{q}_h \cdot \boldsymbol{n}_\Gamma(\overline{\boldsymbol{x}}) - \boldsymbol{q}_h \cdot \boldsymbol{n}_{\Gamma_h}(\boldsymbol{x})| + |g(\overline{\boldsymbol{x}})| + \kappa l(\boldsymbol{x})^{1/2} \left(\int_0^{l(\boldsymbol{x})} |\boldsymbol{q}_h(\boldsymbol{x} + \boldsymbol{t}(\boldsymbol{x})s)|^2 ds \right)^{1/2},$$

and, given $e \in \mathcal{E}_\Gamma$ and $\boldsymbol{x} \in e$, we have

$$\int_e |\varphi_h(\boldsymbol{x})|^2 d\boldsymbol{x} \leq \frac{1}{3} \int_e |\boldsymbol{q}_h \cdot \boldsymbol{n}_\Gamma(\overline{\boldsymbol{x}}) - \boldsymbol{q}_h \cdot \boldsymbol{n}_{\Gamma_h}(\boldsymbol{x})|^2 d\boldsymbol{x} + \frac{1}{3} \int_e |g(\overline{\boldsymbol{x}})|^2 d\boldsymbol{x} + \frac{1}{3}\kappa^2 \left|\!\left|\!\left| l^{1/2} \boldsymbol{q}_h \right|\!\right|\!\right|_e^2, \tag{24}$$

by the definition in (2).

Since $\boldsymbol{\phi}$ is bijective, from (24) and (6), we obtain

$$\begin{aligned}
\|\varphi_h\|_e^2 &\leq \frac{1}{3}\|(\boldsymbol{q}_h \cdot \boldsymbol{n}_\Gamma) \circ \boldsymbol{\phi} - \boldsymbol{q}_h \cdot \boldsymbol{n}_{\Gamma_h}\|_e^2 + \frac{1}{3}\|g \circ \boldsymbol{\phi}\|_e^2 + \frac{1}{3}\kappa^2 \delta_e |\!|\!| \boldsymbol{q}_h |\!|\!|_e^2 \\
&\leq \frac{1}{3}\|(\boldsymbol{q}_h \cdot \boldsymbol{n}_\Gamma) \circ \boldsymbol{\phi} - \boldsymbol{q}_h \cdot \boldsymbol{n}_{\Gamma_h}\|_e^2 + \frac{1}{3}\|g \circ \boldsymbol{\phi}\|_e^2 + \frac{1}{3}\kappa^2 (C_{ext}^e)^2 \delta_e^2 (h_e^\perp)^{-1} \|\boldsymbol{q}_h\|_{K_e}^2,
\end{aligned}$$

from which, after adding and subtracting $\boldsymbol{q}_h \cdot \boldsymbol{n}_{\Gamma_h}$, it follows that

$$\begin{aligned}
\|\varphi_h\|_e^2 \leq &\frac{1}{6}\|(\boldsymbol{q}_h \cdot \boldsymbol{n}_{\Gamma_h}) \circ \boldsymbol{\phi} - \boldsymbol{q}_h \cdot \boldsymbol{n}_{\Gamma_h}\|_e^2 + \frac{1}{6}\|(\boldsymbol{q}_h \cdot \boldsymbol{n}_\Gamma) \circ \boldsymbol{\phi} - (\boldsymbol{q}_h \cdot \boldsymbol{n}_{\Gamma_h}) \circ \boldsymbol{\phi}\|_e^2 \\
&+ \frac{1}{3}\|g \circ \boldsymbol{\phi}\|_e^2 + \frac{1}{3}\kappa^2 (C_{ext}^e)^2 \delta_e^2 (h_e^\perp)^{-1} \|\boldsymbol{q}_h\|_{K_e}^2
\end{aligned}$$

and by Lemma 5,

$$\begin{aligned}
\|\varphi_h\|_e^2 \leq &\frac{1}{6}(C_{ext}^e)^2 \delta_e^2 h_e^{-3} \|\boldsymbol{q}_h\|_{K_e}^2 + \frac{1}{6}\|(\boldsymbol{q}_h \cdot \boldsymbol{n}_\Gamma) \circ \boldsymbol{\phi} - (\boldsymbol{q}_h \cdot \boldsymbol{n}_{\Gamma_h}) \circ \boldsymbol{\phi}\|_e^2 \\
&+ \frac{1}{3}\|g \circ \boldsymbol{\phi}\|_e^2 + \frac{1}{3}\kappa^2 (C_{ext}^e)^2 \delta_e^2 (h_e^\perp)^{-1} \|\boldsymbol{q}_h\|_{K_e}^2.
\end{aligned} \tag{25}$$

Since $\Gamma_e = \boldsymbol{\phi}(e)$, (25) can be rewritten as

$$\begin{aligned}
\|\varphi_h\|_e^2 \leq &\frac{1}{6}(C_{ext}^e)^2 \delta_e^2 h_e^{-3} \|\boldsymbol{q}_h\|_{K_e}^2 + \frac{1}{6}\|\boldsymbol{q}_h \cdot (\boldsymbol{n}_\Gamma - \boldsymbol{n}_{\Gamma_h})\|_{\Gamma_e}^2 + \frac{1}{3}\|g\|_{\Gamma_e}^2 + \frac{1}{3}\kappa^2 (C_{ext}^e)^2 \delta_e^2 (h_e^\perp)^{-1} \|\boldsymbol{q}_h\|_{K_e}^2 \\
\leq &\frac{1}{6}(C_{ext}^e)^2 \delta_e^2 h_e^{-3} \|\boldsymbol{q}_h\|_{K_e}^2 + \frac{1}{6}\|\boldsymbol{q}_h\|_{\Gamma_e}^2 \|\boldsymbol{n}_\Gamma - \boldsymbol{n}_{\Gamma_h}\|_{\infty,\Gamma_e}^2 + \frac{1}{3}\|g\|_{\Gamma_e}^2 + \frac{1}{3}\kappa^2 (C_{ext}^e)^2 \delta_e^2 (h_e^\perp)^{-1} \|\boldsymbol{q}_h\|_{K_e}^2
\end{aligned}$$

and by considering that $\mathcal{T}_h$ is an admissible triangulation, we have that

$$\|\varphi_h\|_e^2 \leq \frac{1}{6}(C_{ext}^e)^2 \delta_e^2 h_e^{-3} \|\boldsymbol{q}_h\|_{K_e}^2 + \frac{1}{6} C_\Gamma^2 \delta_e^{2\alpha} \|\boldsymbol{q}_h\|_{\Gamma_e}^2 + \frac{1}{3}\|g\|_{\Gamma_e}^2 + \frac{1}{3}\kappa^2 (C_{ext}^e)^2 \delta_e^2 (h_e^\perp)^{-1} \|\boldsymbol{q}_h\|_{K_e}^2.$$

Now, by the discrete trace inequality (18), (3), (5) and (6), we obtain

$$\|\boldsymbol{q}_h\|_{\Gamma_e} \leq C_{\Gamma_e}^{tr} \delta_e^{-1/2} \|\boldsymbol{q}_h\|_{K_{ext}^e} \leq C_2^e C_{\Gamma_e}^{tr} \delta_e^{-1/2} |\!|\!| \boldsymbol{q}_h |\!|\!|_e \leq C_{ext}^e C_2^e C_{\Gamma_e}^{tr} (h_e^\perp)^{-1/2} \|\boldsymbol{q}_h\|_{K_e}.$$

Finally, the last two inequalities and the fact that $h_e \leq \gamma h_e^\perp$, imply (22). □

From the Gårding-type identity (20) and the bound for φ_h in (7), we can observe that a smallness assumption on $C_{\delta,\kappa,h}$ will be required:

(A.1) $C_{\delta,\kappa,h}\kappa^{-1} \leq \dfrac{3}{200}$.

Remark 8. *This assumption provides a condition that relates the distance δ between Γ_h and Γ with the meshsize h and wavenumber κ. For instance, in virtue of Remark 1, if $\alpha = 1/2$ and δ is of order h^2, by performing some calculations we observe that (A.1) holds true if $h\kappa^{-1}(1+\kappa^2 h^2)$ is sufficiently small. In particular, this is true when $h\kappa \lesssim 1$. On the other hand, in the case of Ω being polyhedral, we mean $\Omega = \Omega_h$, δ would be zero and therefore $C_{\delta,\kappa,h}$ too.*

We now employ the Gårding identity in order to obtain estimates for $\boldsymbol{q}_h$, $\tau^{1/2}(u_h - \widehat{u}_h)$ and $\widehat{u}_h$ in terms of the source terms and scalar unknown u_h. The latter ones will be controlled afterwards by a duality argument.

It is convenient to define the following quantity related to the sources of the problem:

$$S(f, g, \boldsymbol{G}, G_\partial, \kappa) := \kappa^{-2}\|f\|^2_{\mathcal{T}_h} + \kappa^{-1}\|g\|^2_{\Gamma} + \|\boldsymbol{G}\|^2_{\mathcal{T}_h} + \kappa^{-1}\|G_\partial\|^2_{\Gamma_h}. \tag{26}$$

Since we are interested in analyzing the case of large wavenumbers, for $\kappa \geq 1$ we notice that $S(f, g, \boldsymbol{G}, G_\partial, \kappa) \leq S(f, g, \boldsymbol{G}, G_\partial, 1)$.

Lemma 9. *Let us assume (A.1) holds. There exist positive constants C_1 and C_2, independent of h, κ and δ such that the solution $(\boldsymbol{q}_h, u_h, \widehat{u}_h) \in \boldsymbol{V}_h \times W_h \times M_h$ of (10) satisfies*

$$\|\boldsymbol{q}_h\|^2_{\mathcal{T}_h} \leq \frac{6}{5}\kappa^2\|u_h\|^2_{\mathcal{T}_h} + C_1 S(f, g, \boldsymbol{G}, G_\partial, \kappa) \tag{27a}$$

and

$$\|\tau^{1/2}(u_h - \widehat{u}_h)\|^2_{\partial\mathcal{T}_h} + \frac{\kappa}{2}\|\widehat{u}_h\|^2_{\Gamma_h} \leq \frac{\kappa^2}{20}\|u_h\|^2_{\mathcal{T}_h} + C_2 S(f, g, \boldsymbol{G}, G_\partial, \kappa). \tag{27b}$$

Proof. Taking real part in (20) and using Young's inequality, we deduce that

$$\frac{199}{200}\|\boldsymbol{q}_h\|^2_{\mathcal{T}_h} \leq \kappa^2\left(1 + \frac{1}{12}\right)\|u_h\|^2_{\mathcal{T}_h} + \frac{\kappa^{-1}}{2}\|\varphi_h + G_\partial\|^2_{\Gamma_h} + \frac{\kappa}{2}\|\widehat{u}_h\|^2_{\Gamma_h} + 50\|\boldsymbol{G}\|^2_{\mathcal{T}_h} + 3\kappa^{-2}\|f\|^2_{\mathcal{T}_h}$$

and combining this inequality with the estimate in (22), it follows

$$\begin{aligned}\left(\frac{199}{200} - \frac{1}{3}C_{\delta,\kappa,h}\kappa^{-1}\right)\|\boldsymbol{q}_h\|^2_{\mathcal{T}_h} \leq& \kappa^2\frac{13}{12}\|u_h\|^2_{\mathcal{T}_h} + \kappa^{-1}\|G_\partial\|^2_{\Gamma_h} + 50\|\boldsymbol{G}\|^2_{\mathcal{T}_h} \\ &+ 3\kappa^{-2}\|f\|^2_{\mathcal{T}_h} + \frac{\kappa^{-1}}{3}\|g\|^2_{\Gamma_h} + \frac{\kappa}{2}\|\widehat{u}_h\|^2_{\Gamma_h}.\end{aligned}$$

Then, by Assumption (A.1), $C_{\delta,\kappa,h}\kappa^{-1} \leq 3/200$; and definition (26), we have

$$\frac{99}{100}\|\boldsymbol{q}_h\|^2_{\mathcal{T}_h} \leq \frac{13\kappa^2}{12}\|u_h\|^2_{\mathcal{T}_h} + \frac{\kappa}{2}\|\widehat{u}_h\|^2_{\Gamma_h} + 50 S(f, g, \boldsymbol{G}, G_\partial, \kappa). \tag{28}$$

On the other hand, considering the imaginary part in (20) and Young's inequality with parameters $\epsilon_2 > 0$ and $\epsilon_4 > 0$ at our disposal; and the estimate (22), we obtain

$$\begin{aligned}\|\tau^{1/2}(u_h - \widehat{u}_h)\|^2_{\partial\mathcal{T}_h} + \frac{\kappa}{2}\|\widehat{u}_h\|^2_{\Gamma_h} \leq& \frac{\epsilon_2}{2}\|u_h\|^2_{\mathcal{T}_h} + \frac{\kappa^{-1}}{2}\|\varphi_h + G_\partial\|^2_{\Gamma_h} + \frac{1}{2\epsilon_4}\|\boldsymbol{G}\|^2_{\mathcal{T}_h} + \frac{\epsilon_4}{2}\|\boldsymbol{q}_h\|^2_{\mathcal{T}_h} + \frac{1}{2\epsilon_2}\|f\|^2_{\mathcal{T}_h} \\ \leq& \frac{\epsilon_2}{2}\|u_h\|^2_{\mathcal{T}_h} + \kappa^{-1}\|G_\partial\|^2_{\Gamma_h} + \left(\frac{\epsilon_4}{2} + \frac{\kappa^{-1}}{3}C_{\delta,\kappa,h}\right)\|\boldsymbol{q}_h\|^2_{\mathcal{T}_h} \\ &+ \frac{\kappa^{-1}}{3}\|g\|^2_{\Gamma} + \frac{1}{2\epsilon_4}\|\boldsymbol{G}\|^2_{\mathcal{T}_h} + \frac{1}{2\epsilon_2}\|f\|^2_{\mathcal{T}_h},\end{aligned} \tag{29}$$

from which, by taking $\epsilon_2 = \kappa^2/6$, $\epsilon_4 = 4/225$ and noticing that $C_{\delta,\kappa,h}\kappa^{-1} \leq 3/200 \leq 6/225$, by Assumption (A.1), we deduce that there exists $C > 0$, independent of h and κ, such that

$$\|\tau^{1/2}(u_h - \widehat{u}_h)\|^2_{\partial\mathcal{T}_h} + \frac{\kappa}{2}\|\widehat{u}_h\|^2_{\Gamma_h} \leq \frac{\kappa^2}{12}\|u_h\|^2_{\mathcal{T}_h} + \frac{4}{225}\|\boldsymbol{q}_h\|^2_{\mathcal{T}_h} + CS(f, g, \boldsymbol{G}, G_\partial, \kappa).$$

Then, by using this expression to bound the second term in (28), we conclude (27a).
Now, if we choose $\epsilon_2 = \kappa^2/25$, $\epsilon_4 = 1/25$ in (29), we have

$$\begin{aligned}\|\tau^{1/2}(u_h - \widehat{u}_h)\|^2_{\partial\mathcal{T}_h} + \frac{\kappa}{2}\|\widehat{u}_h\|^2_{\Gamma_h} \leq & \frac{\kappa^2}{50}\|u_h\|^2_{\mathcal{T}_h} + \kappa^{-1}\|G_\partial\|^2_{\Gamma_h} + \left(\frac{1}{50} + \frac{\kappa^{-1}}{3}C_{\delta,\kappa,h}\right)\|\boldsymbol{q}_h\|^2_{\mathcal{T}_h} \\ & + \frac{\kappa^{-1}}{3}\|g\|^2_\Gamma + \frac{25}{2}\|\boldsymbol{G}\|^2_{\mathcal{T}_h} + \frac{25}{2}\kappa^{-2}\|f\|^2_{\mathcal{T}_h},\end{aligned}$$

which implies (27b), according with the bounds given in (27a) and Assumption (A.1). □

4.3 Duality argument.

In this section we will employ a duality argument in order to bound $\|u_h\|_{\mathcal{T}_h}$. We consider that, given $\Theta \in \mathrm{L}^2(\Omega)$, the solution to the auxiliary problem

$$\boldsymbol{\Phi} + \nabla\psi = 0 \quad \text{in } \Omega, \tag{30a}$$

$$\nabla\cdot\boldsymbol{\Phi} - \kappa^2\psi = \Theta \quad \text{in } \Omega, \tag{30b}$$

$$-\boldsymbol{\Phi}\cdot\boldsymbol{n}_\Gamma - i\kappa\psi = 0 \quad \text{on } \Gamma, \tag{30c}$$

satisfies the regularity estimate

$$\kappa\|\psi\|_{L^2(\Omega)} + |\psi|_{H^1(\Omega)} + \kappa^{-1}|\psi|_{H^2(\Omega)} \leq C_{reg}\|\Theta\|_\Omega, \tag{31}$$

where C_{reg} is independent of κ. This estimate holds true, for example, in the case of smooth star-shaped domains [14, 17]. In addition, since the auxiliary problem is posed in Ω and the HDG sheme is defined in Ω_h, we consider the following smallness assumptions that relates the regularity constant C_{reg} with the meshsize h, distance δ and wavenumber κ:

(D.1) $D_1\, C_{reg} h\kappa^3(h + \tau_{min}^{-1}) \leq \frac{1}{2}$, where $D_1 > 0$ is a constant, independent of h and κ, that appears in the proof of Corollary 11.1.

(D.2) $D_2 C_{reg}^2\kappa^2\left(h^2(1 + h^2\tau_{max}^2) + C_{\delta,\kappa,h} + \delta^{\min\{1,2\alpha\}}\right) \leq 1/2$, where $D_2 > 0$ is a constant, independent of h and κ, that will appear in the proof of Theorem 13.

We observe that Assumption (D.1) is satisfied for h small enough, whereas (D.2) is fulfilled, for instance, when $\alpha = 1/2$ and δ is of order h^2, as it was mentioned in Remark 8.

Now, an important observation regarding the auxiliary problem, is the fact that the equation (30c) is posed in the boundary Γ. However, as it will be seen in Lemma 11, we will need to deal with terms in Γ_h. Hence, we present the following result that provides a bound of $-\boldsymbol{\Phi}\cdot\boldsymbol{n}_{\Gamma_h} - i\kappa\psi$ on Γ_h, in terms of the local closeness parameter δ_e and Θ.

Proposition 10. *Let $\varphi_\Theta := -\boldsymbol{\Phi}\cdot\boldsymbol{n}_{\Gamma_h} - i\kappa\psi$ on Γ_h. It holds,*

$$\|\varphi_\Theta\|^2_{\Gamma_h} \leq 3\, C_{reg}^2 \max_{e\in\mathcal{E}_\Gamma}\left((1+\kappa^2)\delta_e + C_\Gamma^2\,\delta_e^{2\alpha}\right)\|\Theta\|^2_\Omega. \tag{32}$$

Proof. Let $e \in \mathcal{E}_\Gamma$ and $\boldsymbol{x} \in e$ with its corresponding $\overline{\boldsymbol{x}} \in \Gamma$. The same argument employed to obtain (9) yields, after adding and subtracting $\boldsymbol{\Phi}(\boldsymbol{x}) \cdot \boldsymbol{n}_\Gamma(\overline{\boldsymbol{x}})$,

$$\varphi_\Theta(\boldsymbol{x}) = \boldsymbol{\Phi} \cdot \boldsymbol{n}_\Gamma(\overline{\boldsymbol{x}}) - \boldsymbol{\Phi}(\boldsymbol{x}) \cdot \boldsymbol{n}_\Gamma(\overline{\boldsymbol{x}}) + \boldsymbol{\Phi}(\boldsymbol{x}) \cdot \boldsymbol{n}_\Gamma(\overline{\boldsymbol{x}}) - \boldsymbol{\Phi} \cdot \boldsymbol{n}_{\Gamma_h}(\boldsymbol{x}) + i\,\kappa \int_0^{l(\boldsymbol{x})} \boldsymbol{\Phi}(\boldsymbol{x} + \boldsymbol{t}(\boldsymbol{x})s) \cdot \boldsymbol{t}(\boldsymbol{x})\, ds.$$

Then,

$$\|\varphi_\Theta\|_{\Gamma_h}^2 \leq 3\,\|\boldsymbol{\Phi} \circ \boldsymbol{\phi} - \boldsymbol{\Phi}\|_{\Gamma_h}^2 + 3\,\|\boldsymbol{\Phi}\|_{\Gamma_h}^2 \|\boldsymbol{n}_\Gamma - \boldsymbol{n}_{\Gamma_h}\|_{\infty,\Gamma_e}^2 + 3\,\kappa^2 \sum_{e \in \mathcal{E}_\Gamma} \left|\left|\left| l^{1/2} \boldsymbol{\Phi} \right|\right|\right|_e^2.$$

Now, by (31) and considering the fact that $\mathcal{T}_h$ is an admissible triangulation, we obtain

$$\|\varphi_\Theta\|_{\Gamma_h}^2 \leq 3\,\|\boldsymbol{\Phi} \circ \boldsymbol{\phi} - \boldsymbol{\Phi}\|_{\Gamma_h}^2 + 3\,C_{reg}^2\,\|\Theta\|_\Omega^2 \max_{e \in \mathcal{E}_\Gamma} C_\Gamma^2\,\delta_e^{2\alpha} + 3\,C_{reg}^2\,\kappa^2 \max_{e \in \mathcal{E}_\Gamma} \delta_e\,\|\Theta\|_\Omega^2,$$

where we have used the fact that for $\boldsymbol{x} \in e$, $l(\boldsymbol{x}) \leq \delta_e$.
Finally, by Lemma 1 in [21], we have that $\|\boldsymbol{\Phi} \circ \boldsymbol{\phi} - \boldsymbol{\Phi}\|_{\Gamma_h}^2 \leq \delta_e |\boldsymbol{\Phi}|_{\boldsymbol{H}^1(\Omega)}^2$ and the result follows. $\square$

Lemma 11. *Let $(\boldsymbol{\Phi}, \psi) \in \boldsymbol{H}(\boldsymbol{div}, \Omega) \times H^1(\Omega)$ and $(\boldsymbol{q}_h, u_h, \widehat{u}_h) \in \boldsymbol{V}_h \times W_h \times M_h$ be the solutions of (30) and (10), respectively. If $k \geq 1$, for any $\psi_{k-1} \in \mathcal{P}_{k-1}(\mathcal{T}_h)$ and any $\boldsymbol{\Phi}_{k-1} \in \mathbf{P}_{k-1}(\mathcal{T}_h)$, there holds*

$$\begin{aligned}(u_h, \Theta)_{\mathcal{T}_h} = &(\boldsymbol{q}_h, \Pi_{\boldsymbol{V}}^* \boldsymbol{\Phi} - \boldsymbol{\Phi})_{\mathcal{T}_h} + (u_h, \kappa^2(\Pi_W^* \psi - \psi))_{\mathcal{T}_h} - (\boldsymbol{G}, \Pi_{\boldsymbol{V}}^* \boldsymbol{\Phi} - \boldsymbol{\Phi}_{k-1})_{\mathcal{T}_h} \\ &+ (f, \Pi_W^* \psi - \psi_{k-1})_{\mathcal{T}_h} + (f, \psi_{k-1})_{\mathcal{T}_h} - \langle \widehat{u}_h, \varphi_\Theta \rangle_{\Gamma_h} + \langle \varphi_h + G_\partial, P_{M_h} \psi \rangle_{\Gamma_h}.\end{aligned} \tag{33}$$

Proof. First let us test (30b) with u_h and after using integration by parts, the orthogonality of Π_h^* and (12a) with $\boldsymbol{v} = \Pi_{\boldsymbol{V}}^* \boldsymbol{\Phi}$, we obtain

$$\begin{aligned}(u_h, \Theta)_{\mathcal{T}_h} &= (u_h, \nabla \cdot \boldsymbol{\Phi})_{\mathcal{T}_h} - (u_h, \kappa^2 \psi)_{\mathcal{T}_h} \\ &= -(\nabla u_h, \boldsymbol{\Phi})_{\mathcal{T}_h} + \langle u_h, \boldsymbol{\Phi} \cdot \boldsymbol{n}_{\Gamma_h} \rangle_{\partial \mathcal{T}_h} - (u_h, \kappa^2 \psi)_{\mathcal{T}_h} \\ &= -(\nabla u_h, \Pi_{\boldsymbol{V}}^* \boldsymbol{\Phi})_{\mathcal{T}_h} + \langle u_h, \boldsymbol{\Phi} \cdot \boldsymbol{n}_{\Gamma_h} \rangle_{\partial \mathcal{T}_h} - (u_h, \kappa^2 \psi)_{\mathcal{T}_h} \\ &= (u_h, \nabla \cdot \Pi_{\boldsymbol{V}}^* \boldsymbol{\Phi})_{\mathcal{T}_h} - \langle u_h, (\Pi_{\boldsymbol{V}}^* \boldsymbol{\Phi} - \boldsymbol{\Phi}) \cdot \boldsymbol{n}_{\Gamma_h} \rangle_{\partial \mathcal{T}_h} - (u_h, \kappa^2 \psi)_{\mathcal{T}_h} \\ &= (\boldsymbol{q}_h, \Pi_{\boldsymbol{V}}^* \boldsymbol{\Phi})_{\mathcal{T}_h} - (\boldsymbol{G}, \Pi_{\boldsymbol{V}}^* \boldsymbol{\Phi})_{\mathcal{T}_h} + \langle \widehat{u}_h, \Pi_{\boldsymbol{V}}^* \boldsymbol{\Phi} \cdot \boldsymbol{n}_{\Gamma_h} \rangle_{\partial \mathcal{T}_h} - \langle u_h, (\Pi_{\boldsymbol{V}}^* \boldsymbol{\Phi} - \boldsymbol{\Phi}) \cdot \boldsymbol{n}_{\Gamma_h} \rangle_{\partial \mathcal{T}_h} \\ &\quad - (u_h, \kappa^2 \psi)_{\mathcal{T}_h}.\end{aligned} \tag{34}$$

Now, by using (10b), (30a) and integration by parts, we have

$$\begin{aligned}-(u_h, \kappa^2 \psi)_{\mathcal{T}_h} &= -(u_h, \kappa^2 \Pi_W^* \psi)_{\mathcal{T}_h} - (u_h, \kappa^2(\psi - \Pi_W^* \psi))_{\mathcal{T}_h} \\ &= (\boldsymbol{q}_h, \nabla \Pi_W^* \psi)_{\mathcal{T}_h} - \langle \widehat{\boldsymbol{q}}_h \cdot \boldsymbol{n}_{\Gamma_h}, \Pi_W^* \psi \rangle_{\partial \mathcal{T}_h} + (f, \Pi_W^* \psi)_{\mathcal{T}_h} - (u_h, \kappa^2(\psi - \Pi_W^* \psi))_{\mathcal{T}_h} \\ &= -(\nabla \cdot \boldsymbol{q}_h, \Pi_W^* \psi)_{\mathcal{T}_h} - \langle (\widehat{\boldsymbol{q}}_h - \boldsymbol{q}_h) \cdot \boldsymbol{n}_{\Gamma_h}, \Pi_W^* \psi \rangle_{\partial \mathcal{T}_h} + (f, \Pi_W^* \psi)_{\mathcal{T}_h} \\ &\quad - (u_h, \kappa^2(\psi - \Pi_W^* \psi))_{\mathcal{T}_h} \\ &= -(\nabla \cdot \boldsymbol{q}_h, \psi)_{\mathcal{T}_h} - \langle (\widehat{\boldsymbol{q}}_h - \boldsymbol{q}_h) \cdot \boldsymbol{n}_{\Gamma_h}, \Pi_W^* \psi \rangle_{\partial \mathcal{T}_h} + (f, \Pi_W^* \psi)_{\mathcal{T}_h} - (u_h, \kappa^2(\psi - \Pi_W^* \psi))_{\mathcal{T}_h} \\ &= (\boldsymbol{q}_h, \nabla \psi)_{\mathcal{T}_h} - \langle \boldsymbol{q}_h \cdot \boldsymbol{n}_{\Gamma_h}, \psi \rangle_{\partial \mathcal{T}_h} - \langle (\widehat{\boldsymbol{q}}_h - \boldsymbol{q}_h) \cdot \boldsymbol{n}_{\Gamma_h}, \Pi_W^* \psi \rangle_{\partial \mathcal{T}_h} + (f, \Pi_W^* \psi)_{\mathcal{T}_h} \\ &\quad - (u_h, \kappa^2(\psi - \Pi_W^* \psi))_{\mathcal{T}_h} \\ &= -(\boldsymbol{q}_h, \boldsymbol{\Phi})_{\mathcal{T}_h} - \langle \widehat{\boldsymbol{q}}_h \cdot \boldsymbol{n}_{\Gamma_h}, \psi \rangle_{\partial \mathcal{T}_h} + \langle (\widehat{\boldsymbol{q}}_h - \boldsymbol{q}_h) \cdot \boldsymbol{n}_{\Gamma_h}, \psi - \Pi_W^* \psi \rangle_{\partial \mathcal{T}_h} + (f, \Pi_W^* \psi)_{\mathcal{T}_h} \\ &\quad - (u_h, \kappa^2(\psi - \Pi_W^* \psi))_{\mathcal{T}_h} \\ &= -(\boldsymbol{q}_h, \boldsymbol{\Phi})_{\mathcal{T}_h} - \langle \widehat{\boldsymbol{q}}_h \cdot \boldsymbol{n}_{\Gamma_h}, \psi \rangle_{\Gamma_h} + \langle i\tau(u_h - \widehat{u}_h), \psi - \Pi_W^* \psi \rangle_{\partial \mathcal{T}_h} + (f, \Pi_W^* \psi)_{\mathcal{T}_h} \\ &\quad - (u_h, \kappa^2(\psi - \Pi_W^* \psi))_{\mathcal{T}_h}.\end{aligned}$$

Moreover, since $\langle \widehat{u}_h, \Pi_{\boldsymbol{V}}^* \boldsymbol{\Phi} \cdot \boldsymbol{n}_{\Gamma_h} \rangle_{\partial \mathcal{T}_h} = \langle \widehat{u}_h, (\Pi_{\boldsymbol{V}}^* \boldsymbol{\Phi} - \boldsymbol{\Phi}) \cdot \boldsymbol{n}_{\Gamma_h} \rangle_{\partial \mathcal{T}_h} + \langle \widehat{u}_h, \boldsymbol{\Phi} \cdot \boldsymbol{n}_{\Gamma_h} \rangle_{\Gamma_h}$, substituting both equalities in (34) and using (13), we obtain

$$\begin{aligned}(u_h, \Theta)_{\mathcal{T}_h} =& (\boldsymbol{q}_h, \Pi_{\boldsymbol{V}}^* \boldsymbol{\Phi} - \boldsymbol{\Phi})_{\mathcal{T}_h} - \langle u_h - \widehat{u}_h, (\Pi_{\boldsymbol{V}}^* \boldsymbol{\Phi} - \boldsymbol{\Phi}) \cdot \boldsymbol{n}_{\Gamma_h} - i\tau(\Pi_W^* \psi - \psi) \rangle_{\partial \mathcal{T}_h} \\ & - (u_h, \kappa^2(\psi - \Pi_W^* \psi))_{\mathcal{T}_h} - (\boldsymbol{G}, \Pi_{\boldsymbol{V}}^* \boldsymbol{\Phi})_{\mathcal{T}_h} + (f, \Pi_W^* \psi)_{\mathcal{T}_h} + \langle \widehat{u}_h, \boldsymbol{\Phi} \cdot \boldsymbol{n}_{\Gamma_h} \rangle_{\Gamma_h} - \langle \widehat{\boldsymbol{q}}_h \cdot \boldsymbol{n}_{\Gamma_h}, \psi \rangle_{\Gamma_h}.\end{aligned}$$

By using the definition of φ_Θ given in Proposition 10, we rewrite the last two terms as follows

$$\langle \widehat{u}_h, \boldsymbol{\Phi} \cdot \boldsymbol{n}_{\Gamma_h} \rangle_{\Gamma_h} - \langle \widehat{\boldsymbol{q}}_h \cdot \boldsymbol{n}_{\Gamma_h}, \psi \rangle_{\Gamma_h} = - \langle \widehat{u}_h, \varphi_\Theta \rangle_{\Gamma_h} + \langle -\widehat{\boldsymbol{q}}_h \cdot \boldsymbol{n}_{\Gamma_h} + i\kappa \widehat{u}_h, \psi \rangle_{\Gamma_h},$$

which implies (33), according with the orthogonality properties of P_{M_h}, (12b) and the fact that $\boldsymbol{G}$ is orthogonal to functions in $\mathbf{P}_{k-1}(\mathcal{T}_h)$. □

Finally, for the identity in Lemma 11, the boubd in (10) and the approximation properties of the HDG projection, we conclude the following estimate for the L^2 norm of u_h:

Corollary 11.1. *Let $(\boldsymbol{\Phi}, \psi) \in \boldsymbol{H}(\boldsymbol{div}, \Omega) \times H^1(\Omega)$ and $(\boldsymbol{q}_h, u_h, \widehat{u}_h) \in \boldsymbol{V}_h \times W_h \times M_h$ the solutions of* (30) *and* (10)*, respectively. For $k \geq 1$, under the Assumption (D.1) and the regularity estimate* (31)*, it holds*

$$\begin{aligned}\kappa \|u_h\|_{\mathcal{T}_h} \lesssim C_{reg}\, \kappa \Big(\Big(h + h^2 \tau_{max} + C_{\delta,\kappa,h}^{1/2} \Big) \|\boldsymbol{q}_h\|_{\mathcal{T}_h} + (1+\kappa) \delta^{\min\{1/2, \alpha\}} \|\widehat{u}_h\|_{\Gamma_h} \\ + \kappa h (1 + h\tau_{max}) \|\boldsymbol{G}\|_{\mathcal{T}_h} + (\kappa h (h + \tau_{min}^{-1}) + h + \kappa^{-1}) \|f\|_{\mathcal{T}_h} + \|g\|_{\Gamma_h} + \|G_\partial\|_{\Gamma_h} \Big).\end{aligned} \tag{35}$$

Remark 12. *In the particular case that f is orthogonal to piecewise polynomials of degree $k-1$, the term multiplying $\|f\|_{\mathcal{T}_h}$ becomes $\kappa h(h + \tau_{min}^{-1}) + h$, as we will see in the proof.*

Proof. We bound each term of the right hand side of (33) by applying Cauchy-Schwarz inequality, (31) and (22) as follows. For the first term we employ approximation property (15a) in the context of the projector $\Pi_{\boldsymbol{V}}^*$:

$$|(\boldsymbol{q}_h, \Pi_{\boldsymbol{V}}^* \boldsymbol{\Phi} - \boldsymbol{\Phi})_{\mathcal{T}_h}| \lesssim C_{reg} h (1 + h\tau_{max}) \|\boldsymbol{q}_h\|_{\mathcal{T}_h} \|\Theta\|_\Omega.$$

Similarly for the second term, but considering (15b) for Π_W^* and recalling that $\kappa \geq 1$,

$$|(u_h, \kappa^2(\Pi_W^* \psi - \psi))_{\mathcal{T}_h}| \lesssim C_{reg} h \kappa^3 (h + \tau_{min}^{-1}) \|u_h\|_{\mathcal{T}_h} \|\Theta\|_\Omega.$$

Then, for the third term we write

$$\begin{aligned}|(\boldsymbol{G}, \Pi_{\boldsymbol{V}}^* \boldsymbol{\Phi} - \boldsymbol{\Phi}_{k-1})_{\mathcal{T}_h}| &\leq |(\boldsymbol{G}, \Pi_{\boldsymbol{V}}^* \boldsymbol{\Phi} - \boldsymbol{\Phi})_{\mathcal{T}_h}| + |(\boldsymbol{G}, \boldsymbol{\Phi} - \boldsymbol{\Phi}_{k-1})_{\mathcal{T}_h}| \\ &\lesssim C_{reg} \kappa h (1 + h\tau_{max}) \|\boldsymbol{G}\|_{\mathcal{T}_h} \|\Theta\|_\Omega + C_{reg} \kappa h \|\boldsymbol{G}\|_{\mathcal{T}_h} \|\Theta\|_\Omega \\ &\lesssim C_{reg} \kappa h (1 + h\tau_{max}) \|\boldsymbol{G}\|_{\mathcal{T}_h} \|\Theta\|_\Omega,\end{aligned}$$

where we have taken $\boldsymbol{\Phi}_{k-1}$ to be the L^2-projection of $\boldsymbol{\Phi}$ into the space $\mathbf{P}_{k-1}(\mathcal{T}_h)$ and used its approximation properties. For the fourth and fifth term, we consider ψ_{k-1} as the L^2-projection of ψ into the space $\mathbb{P}_{k-1}(\mathcal{T}_h)$ and use its approximation properties to deduce that

$$\begin{aligned}|(f, \Pi_W^* \psi - \psi_{k-1})_{\mathcal{T}_h} + (f, \psi_{k-1})_{\mathcal{T}_h}| \leq& |(f, \Pi_W^* \psi - \psi)_{\mathcal{T}_h}| + |(f, \psi - \psi_{k-1})_{\mathcal{T}_h}| + |(f, \psi_{k-1})_{\mathcal{T}_h}| \\ \lesssim& (C_{reg} h \kappa (h + \tau_{min}^{-1}) \|f\|_{\mathcal{T}_h} + C_{reg} h \|f\|_{\mathcal{T}_h}) \|\Theta\|_\Omega \\ & + \|f\|_{\mathcal{T}_h} \|\psi_{k-1}\|_{\mathcal{T}_h} \\ \leq& C_{reg} (h\kappa (h + \tau_{min}^{-1}) + h + \kappa^{-1}) \|f\|_{\mathcal{T}_h} \|\Theta\|_\Omega.\end{aligned}$$

In addition, we observe that the term $(f, \psi_{k-1})_{\mathcal{T}_h}$ would vanish if f is orthogonal to piecewise polynomials of degree $k-1$. Since this is not the case in general, we bound $|(f, \psi_{k-1})_{\mathcal{T}_h}| \lesssim C_{reg}\kappa^{-1}\|f\|_{\mathcal{T}_h}\|\Theta\|_\Omega$. For the sixth term, we use (22) and the fact that $\psi \in H^1(\Omega)$, in order to obtain

$$\begin{aligned}
|\langle \varphi_h + G_\partial, P_{M_h}\psi\rangle_{\Gamma_h}| &\leq \|\varphi_h + G_\partial\|_{\Gamma_h}\|P_{M_h}\psi\|_{\partial\mathcal{T}_h} \\
&\lesssim \|\psi\|_{H^1(\Omega)}\|\varphi_h + G_\partial\|_{\Gamma_h} \\
&\lesssim C_{reg}\left(C_{\delta,\kappa,h}^{1/2}\|\boldsymbol{q}_h\|_{\mathcal{T}_h} + \|g\|_{\Gamma_h} + \|G_\partial\|_{\Gamma_h}\right)\|\Theta\|_\Omega.
\end{aligned}$$

Finally, for the last term (32) implies that

$$|\langle \widehat{u}_h, \varphi_\Theta\rangle_{\Gamma_h}| \lesssim C_{reg}(1+\kappa)\delta^{\min\{1/2,\alpha\}}\|\widehat{u}_h\|_{\Gamma_h}\|\Theta\|_\Omega.$$

Then, if we take $\Theta := \begin{cases} u_h, & \text{in } \Omega_h \\ 0, & \text{in } \Omega\setminus\Omega_h \end{cases}$ in (33) and use the above bounds, it follows that there exists $D_1 > 0$, independent of h and κ, such that

$$\begin{aligned}
\|u_h\|_{\mathcal{T}_h} \leq & D_1 C_{reg}\Big(h\kappa^3(h+\tau_{min}^{-1})\|u_h\|_{\mathcal{T}_h} + \kappa h(1+h\tau_{max})\|\boldsymbol{G}\|_{\mathcal{T}_h} + (1+\kappa)\delta^{\min\{1/2,\alpha\}}\|\widehat{u}_h\|_{\partial\mathcal{T}_h} \\
&+\|G_\partial\|_{\Gamma_h} + \left(h(1+h\tau_{max}) + C_{\delta,\kappa,h}^{1/2}\right)\|\boldsymbol{q}_h\|_{\mathcal{T}_h} + \|g\|_{\Gamma_h} + (\kappa h(h+\tau_{min}^{-1}) + h + \kappa^{-1})\|f\|_{\mathcal{T}_h}\Big),
\end{aligned}$$

which implies (35), according to Assumption (D.1). □

4.4 Stability estimate.

The results presented in the preceding subsection allows us to derive one of the main results of this work, namely, the stability estimate of the unfitted HDG scheme:

Theorem 13. *Let $(\boldsymbol{\Phi}, \psi) \in \boldsymbol{H}(\boldsymbol{div}, \Omega) \times H^1(\Omega)$ the solution of (30) and $(\boldsymbol{q}_h, u_h, \widehat{u}_h) \in \boldsymbol{V}_h \times W_h \times M_h$ the solution of (10). If we suppose Assumptions (A.1), (D.1) and (D.2) hold true, then*

$$\|\boldsymbol{q}_h\|_{\mathcal{T}_h} + \kappa\|u_h\|_{\mathcal{T}_h} \lesssim C_{est}\, S(f, g, \boldsymbol{G}, G_\partial, 1)^{1/2} \tag{36}$$

where $C_{est} = C_{reg}\kappa(\kappa(h + h^2\tau_{max} + h^2 + h\tau_{min}^{-1}) + h + \kappa^{-1}) + 1$.

Remark 14. *According with the observation in Remark 12, if f is orthogonal to piecewise polynomials of degree $k-1$, we have that $C_{est} = C_{reg}\kappa^2\left(h + h^2\tau_{max} + h^2 + \tau_{min}^{-1}h\right) + 1$. Moreover, if $C_{reg}\kappa h \lesssim 1$, then the stability constant reduces to $C_{est} = \kappa(1 + h\tau_{max} + \tau_{min}^{-1})$.*

Proof. First, we square (35) and, by (27a) and (27b), it is deduced that there exists $D_2 > 0$, independent of h and κ, such that

$$\begin{aligned}
\kappa^2\|u_h\|_{\mathcal{T}_h}^2 \leq & D_2\, C_{reg}^2\kappa^2\Big\{\left(h^2(1+h^2\tau_{max}^2) + C_{\delta,\kappa,h} + \delta^{\min\{1,2\alpha\}}\right)\left(\kappa^2\|u_h\|_{\mathcal{T}_h}^2 + S(f,g,\boldsymbol{G},G_\partial,\kappa)\right) \\
&+ h^2\kappa^2(1+h\tau_{max})^2\|\boldsymbol{G}\|_{\mathcal{T}_h}^2 + (\kappa h(h+\tau_{min}^{-1}) + h + \kappa^{-1})^2\|f\|_{\mathcal{T}_h}^2\Big\}.
\end{aligned}$$

Then, according to Assumption (D.2) it follows that

$$\begin{aligned}
\kappa^2\|u_h\|_{\mathcal{T}_h}^2 \lesssim & S(f,g,\boldsymbol{G},G_\partial,\kappa) + C_{reg}^2\kappa^4 h^2(1+h\tau_{max})^2\|\boldsymbol{G}\|_{\mathcal{T}_h}^2 \\
&+ C_{reg}^2\kappa^2(\kappa h(h+\tau_{min}^{-1}) + h + \kappa^{-1})^2\|f\|_{\mathcal{T}_h}^2.
\end{aligned}$$

Therefore, combining this expression with (27a) and (26) we obtain (36). □

5 Error analysis.

In the first part of the error analysis, we define the error of the projection $\boldsymbol{I^q} := \boldsymbol{q} - \Pi_{\boldsymbol{V}}\boldsymbol{q}$, $I^u := u - \Pi_W u$ and the projection of the errors by

$$\boldsymbol{e}_h^{\boldsymbol{q}} := \Pi_{\boldsymbol{V}}\boldsymbol{q} - \boldsymbol{q}_h, \quad e_h^u := \Pi_W u - u_h, \quad e_h^{\widehat{u}} := P_{M_h} u - \widehat{u}_h, \quad \boldsymbol{e}_h^{\widehat{\boldsymbol{q}}} \cdot \boldsymbol{n} := P_{M_h}(\boldsymbol{q} \cdot \boldsymbol{n}) - \widehat{\boldsymbol{q}}_h \cdot \boldsymbol{n}, \tag{37}$$

which satisfy a system of equations, whose structure is justified in the proof of the following lemma.

Lemma 15. *Let $(\boldsymbol{q}, u) \in \boldsymbol{H}(\boldsymbol{div};\Omega) \times H^1(\Omega)$ and $(\boldsymbol{q}_h, u_h, \widehat{u}_h) \in \boldsymbol{V}_h \times W_h \times M_h$ solutions of* (1) *and* (7)*, respectively. Then, the projection of the errors $\boldsymbol{e}_h^{\boldsymbol{q}}$, e_h^u and $e_h^{\widehat{u}}$ satisfy the following system of equations*

$$(\boldsymbol{e}_h^{\boldsymbol{q}}, \boldsymbol{v})_{\mathcal{T}_h} - (e_h^u, \nabla \cdot \boldsymbol{v})_{\mathcal{T}_h} + \langle e_h^{\widehat{u}}, \boldsymbol{v} \cdot \boldsymbol{n} \rangle_{\partial\mathcal{T}_h} = -(\boldsymbol{I^q}, \boldsymbol{v})_{\mathcal{T}_h}, \tag{38a}$$

$$-(\boldsymbol{e}_h^{\boldsymbol{q}}, \nabla w)_{\mathcal{T}_h} + \langle \boldsymbol{e}_h^{\boldsymbol{q}} \cdot \boldsymbol{n}, w \rangle_{\partial\mathcal{T}_h} + i\langle \tau(e_h^u - e_h^{\widehat{u}}), w \rangle_{\partial\mathcal{T}_h} - \kappa^2 (e_h^u, w)_{\mathcal{T}_h} = \kappa^2 (I^u, w)_{\mathcal{T}_h}, \tag{38b}$$

$$\langle \boldsymbol{e}_h^{\widehat{\boldsymbol{q}}} \cdot \boldsymbol{n}, \mu \rangle_{\partial\mathcal{T}_h \setminus \Gamma_h} = 0, \tag{38c}$$

$$\langle -\boldsymbol{e}_h^{\widehat{\boldsymbol{q}}} \cdot \boldsymbol{n} + i\kappa e_h^{\widehat{u}}, \mu \rangle_{\Gamma_h} = \langle \varphi - \varphi_h, \mu \rangle_{\Gamma_h}, \tag{38d}$$

for all $(\boldsymbol{v}, w, \mu) \in \boldsymbol{V}_h \times W_h \times M_h$. Moreover,

$$\boldsymbol{e}_h^{\widehat{\boldsymbol{q}}} \cdot \boldsymbol{n} = \boldsymbol{e}_h^{\boldsymbol{q}} \cdot \boldsymbol{n} + i\tau(e_h^u - e_h^{\widehat{u}}), \quad \text{on } \partial\mathcal{T}_h \tag{38e}$$

and, for $\boldsymbol{x} \in \Gamma_h$, $\varphi(\boldsymbol{x}) - \varphi_h(\boldsymbol{x}) = \varphi_{\boldsymbol{e}}(\boldsymbol{x}) + G_\partial(\boldsymbol{x})$, where

$$\varphi_{\boldsymbol{e}}(\boldsymbol{x}) = \boldsymbol{e}_h^{\boldsymbol{q}} \cdot \boldsymbol{n}(\overline{\boldsymbol{x}}) - \boldsymbol{e}_h^{\boldsymbol{q}} \cdot \boldsymbol{n}_{\Gamma_h}(\boldsymbol{x}) + i\,\kappa \int_0^{l(\boldsymbol{x})} \boldsymbol{e}_h^{\boldsymbol{q}}(\boldsymbol{x} + \boldsymbol{t}(\boldsymbol{x})s) \cdot \boldsymbol{t}(\boldsymbol{x})\, ds$$

and

$$G_\partial(\boldsymbol{x}) = \boldsymbol{I^q} \cdot \boldsymbol{n}(\overline{\boldsymbol{x}}) - \boldsymbol{I^q} \cdot \boldsymbol{n}_{\Gamma_h}(\boldsymbol{x}) + i\,\kappa \int_0^{l(\boldsymbol{x})} \boldsymbol{I^q}(\boldsymbol{x} + \boldsymbol{t}(\boldsymbol{x})s) \cdot \boldsymbol{t}(\boldsymbol{x})\, ds. \tag{39}$$

Proof. Due to the deduction of each equation of (38) is similar, we only show the procedure of (38b). Initially, we use the definitions given in (37) in (10b); and organize the expression

$$\begin{aligned}
&-(\boldsymbol{e}_h^{\boldsymbol{q}}, \nabla w)_{\mathcal{T}_h} + \langle \boldsymbol{e}_h^{\boldsymbol{q}} \cdot \boldsymbol{n}, w \rangle_{\partial\mathcal{T}_h} + i\langle \tau(e_h^u - e_h^{\widehat{u}}), w \rangle_{\partial\mathcal{T}_h} - \kappa^2 (e_h^u, w)_{\mathcal{T}_h} \\
&\quad = -(f, w)_{\mathcal{T}_h} - (\Pi_{\boldsymbol{V}}\boldsymbol{q}, \nabla w)_{\mathcal{T}_h} + \langle \Pi_{\boldsymbol{V}}\boldsymbol{q} \cdot \boldsymbol{n}, w \rangle_{\partial\mathcal{T}_h} + i\langle \tau(\Pi_W u - P_{M_h} u), w \rangle_{\partial\mathcal{T}_h} - \kappa^2 (\Pi_W u, w)_{\mathcal{T}_h}.
\end{aligned}$$

Then, from (13), integration by parts and (1b), we have

$$\begin{aligned}
&-(\boldsymbol{e}_h^{\boldsymbol{q}}, \nabla w)_{\mathcal{T}_h} + \langle \boldsymbol{e}_h^{\boldsymbol{q}} \cdot \boldsymbol{n}, w \rangle_{\partial\mathcal{T}_h} + i\langle \tau(e_h^u - e_h^{\widehat{u}}), w \rangle_{\partial\mathcal{T}_h} - \kappa^2 (e_h^u, w)_{\mathcal{T}_h} \\
&\quad = \langle (\Pi_{\boldsymbol{V}}\boldsymbol{q} - \boldsymbol{q}) \cdot \boldsymbol{n}, w \rangle_{\partial\mathcal{T}_h} + i\langle \tau(\Pi_W u - u), w \rangle_{\partial\mathcal{T}_h} - i\langle \tau(P_{M_h} u - u), w \rangle_{\partial\mathcal{T}_h} - \kappa^2 (\Pi_W u - u, w)_{\mathcal{T}_h},
\end{aligned}$$

from which (38b) is deduced, as a consequence of (13) and the orthogonality of P_{M_h}. $\square$

Theorem 16. *Let us assume $(\boldsymbol{q}, u) \in \boldsymbol{H}^{l_{\boldsymbol{q}}+1}(\mathcal{T}_h) \times H^{l_u+1}(\mathcal{T}_h)$ for $l_{\boldsymbol{q}}, l_u \in [0, k]$. Under the same assumptions of Theorem 13, we have*

$$\begin{aligned}
\|\boldsymbol{e}_h^{\boldsymbol{q}}\|_{\mathcal{T}_h} + \kappa \|e_h^u\|_{\mathcal{T}_h} \lesssim C_{est} \Big(&\|\boldsymbol{I^q}\|_{\mathcal{T}_h} + \kappa \|I^u\|_{\mathcal{T}_h} + \delta^{1/2} |\boldsymbol{I^q}|_{\boldsymbol{H}^1(\Omega)} + \delta^\alpha \|\nabla \boldsymbol{I^q}\|_{\Omega_h^c} \\
&+ (\delta^{\alpha - 1/2} + \kappa\, \delta^{1/2}) \|\boldsymbol{I^q}\|_{\Omega_h^c} \Big).
\end{aligned} \tag{40}$$

Proof. We highlight that the structure of (38) is similar to (10). Then, (36) can be tailored in order to deduce (40). In fact, if we take $g \equiv 0$, $\boldsymbol{G} := -\boldsymbol{I^q}$ and $f := \kappa^2 I^u$ in (36), it follows that

$$\|\boldsymbol{q}_h\|_{\mathcal{T}_h} + \kappa\|u_h\|_{\mathcal{T}_h} \lesssim C_{est}\left(\kappa\|I^u\|_{\mathcal{T}_h} + \|\boldsymbol{I^q}\|_{\mathcal{T}_h} + \kappa^{-1/2}\|G_\partial\|_{\Gamma_h}\right).$$

Now, in order to bound the last term, we take into account the arguments used in the proof of Lemma 7 to deduce that

$$\|G_\partial\|^2_{\Gamma_h} \lesssim \sum_{e\in\mathcal{E}_\Gamma}\left(\|(\boldsymbol{I^q}\circ\phi - \boldsymbol{I^q})\cdot\boldsymbol{n}_\Gamma\|_e^2 + \|(\boldsymbol{I^q}\cdot\boldsymbol{n}_\Gamma)\circ\phi - (\boldsymbol{I^q}\cdot\boldsymbol{n}_{\Gamma_h})\circ\phi\|_e^2 + \kappa^2|\!|\!|l^{1/2}\boldsymbol{I^q}|\!|\!|_e^2\right).$$

Then, by Lemma 5, the fact that $\|\boldsymbol{n}_\Gamma - \boldsymbol{n}_{\Gamma_h}\|_{\infty,\Gamma_e} \le C_\Gamma\,\delta^\alpha$, the norm equivalence given in Lemma 2 and recalling that $l(\boldsymbol{x}) \le \delta$, for all $\boldsymbol{x}\in\Gamma_h$, we have

$$\begin{aligned}\|G_\partial\|^2_{\Gamma_h} \lesssim& \delta|\boldsymbol{I^q}|^2_{\boldsymbol{H}^1(\Omega)} + \sum_{e\in\mathcal{E}_\Gamma}\left(\delta_e^{2\alpha}\|\boldsymbol{I^q}\|^2_{\Gamma_e} + \kappa^2\delta_e\|\boldsymbol{I^q}\|^2_{K^e_{ext}}\right)\\ \lesssim& \delta|\boldsymbol{I^q}|^2_{\boldsymbol{H}^1(\Omega)} + \sum_{e\in\mathcal{E}_\Gamma}\left(\delta_e^{2\alpha}\|\nabla\boldsymbol{I^q}\|^2_{K^e_{ext}} + (\delta_e^{2\alpha-1} + \kappa^2\delta_e)\|\boldsymbol{I^q}\|^2_{K^e_{ext}}\right),\end{aligned}$$

where we have made use of the trace inequality (19). The result follows by recalling that $\kappa \ge 1$. □

Corollary 16.1. *Suppose that $(\boldsymbol{q}, u) \in \boldsymbol{H}^{k+1}(\mathcal{T}_h)\times H^{k+1}(\mathcal{T}_h)$, $\alpha > 1/2$. Under the same assumptions of Theorem 13 and $C_{reg}h\kappa \lesssim 1$. There holds*

$$\|\boldsymbol{q} - \boldsymbol{q}_h\|_{\mathcal{T}_h} + \kappa\|u - u_h\|_{\mathcal{T}_h} \lesssim \kappa h^k(\kappa^2 h + \delta^{1/2}), \tag{41}$$

for τ of order one or κ. Moreover, if $(\boldsymbol{q}, u) \in \boldsymbol{H}^{k+1}(\Omega)\times H^{k+1}(\Omega)$, then $\|\boldsymbol{q} - \boldsymbol{q}_h\|_{\Omega_h^c} + \kappa\|u - u_h\|_{\Omega_h^c}$ is of the same order as $\|\boldsymbol{q} - \boldsymbol{q}_h\|_{\Omega_h} + \kappa\|u - u_h\|_{\Omega_h}$.

Proof. We have that (41) follows from (40), by noticing that $C_{est} \lesssim \kappa$ if τ is of order one or κ, according with Remark 14. Moreover, the last assertion is a straightforward consequence of Theorem 17, (41) and the approximation properties of the HDG projection (15). □

Finally, we also obtain the following estimates of the approximation error outside Ω_h:

Theorem 17. *Let $(\boldsymbol{q}_h, u_h)$ the approximation of $(\boldsymbol{q}, u)$ in Ω_h^c. If $\boldsymbol{q}\in\boldsymbol{H}^{m+1}(\Omega)$ with $m\in[0,k]$, then*

$$\|\boldsymbol{q} - \boldsymbol{q}_h\|_{\Omega_h^c} \lesssim \|\boldsymbol{I^q}\|_{\Omega_h^c} + \|\boldsymbol{e}_h^{\boldsymbol{q}}\|_{\Omega_h}, \tag{42}$$

and

$$\begin{aligned}\kappa\|u - u_h\|_{\Omega_h^c} \lesssim& \delta h^{-3/2}\|\boldsymbol{I^q}\|_{\Omega_h} + (1+\kappa\delta)\|\boldsymbol{I^q}\|_{\Omega_h^c} + (1 + \delta h^{-3/2} + \kappa\delta)\|\boldsymbol{e}_h^{\boldsymbol{q}}\|_{\Omega_h}\\ &+ \delta^{1/2}h^m(1 + \delta^{1/2}h^{-1/2})\|\boldsymbol{q}\|_{\boldsymbol{H}^{m+1}(\Omega)}.\end{aligned}$$

Proof. The first estimate was proved in [9], Lemma 3.7. For the second one, we employ a similar argument as in the proof of Lemma 3.5 in [22].

For the second one, let $e\in\mathcal{E}_\Gamma$, with its corresponding extension patch K^e_{ext} and let us note that by inequality (3), $\|u - u_h\|_{K^e_{ext}} \lesssim |\!|\!|u - u_h|\!|\!|_e$. Now, let $\boldsymbol{y} = \boldsymbol{x} + s\boldsymbol{t}(\boldsymbol{x})$ with $\boldsymbol{x}\in e$ and $s\in[0, l(\boldsymbol{x})]$. Then, from (8), (11) and using the fact that $\overline{\boldsymbol{y}} = \overline{\boldsymbol{x}}$, we have

$$i\kappa(u - u_h)(\boldsymbol{y}) = (\boldsymbol{q} - \boldsymbol{q}_h)\cdot\boldsymbol{n}_\Gamma(\overline{\boldsymbol{x}}) + i\kappa\int_0^{|\overline{\boldsymbol{y}}-\boldsymbol{y}|}(\boldsymbol{q} - \boldsymbol{q}_h)(\boldsymbol{y} + \boldsymbol{t}(\boldsymbol{y})s)\cdot\boldsymbol{t}(\boldsymbol{y})\,ds,$$

which implies that

$$\kappa^2|u-u_h|^2(\boldsymbol{y}) \leq 2\left|(\boldsymbol{q}-\boldsymbol{q}_h)\cdot \boldsymbol{n}_\Gamma(\overline{\boldsymbol{x}})\right|^2 + 2\kappa^2|\overline{\boldsymbol{y}}-\boldsymbol{y}|\int_0^{|\overline{\boldsymbol{y}}-\boldsymbol{y}|}|\boldsymbol{q}-\boldsymbol{q}_h|^2(\boldsymbol{y}+\boldsymbol{t}(\boldsymbol{y})s)ds$$
$$\leq 2\left|(\boldsymbol{q}-\boldsymbol{q}_h)\cdot \boldsymbol{n}_\Gamma(\overline{\boldsymbol{x}})\right|^2 + 2\kappa^2\delta_e\int_0^{l(\boldsymbol{x})}|\boldsymbol{q}-\boldsymbol{q}_h|^2(\boldsymbol{y}+\boldsymbol{t}(\boldsymbol{y})s)ds.$$

Then, integrating over e and $[0, l(\boldsymbol{x})]$, we obtain

$$\begin{aligned}\kappa^2|||u-u_h|||_e^2 \leq & 2\int_e\int_0^{l(\boldsymbol{x})}|(\boldsymbol{q}-\boldsymbol{q}_h)\cdot\boldsymbol{n}_\Gamma(\overline{\boldsymbol{x}})|^2\,ds\,dS_{\boldsymbol{x}} + 2\kappa^2\delta_e\int_e l(\boldsymbol{x})\int_0^{l(\boldsymbol{x})}|\boldsymbol{q}-\boldsymbol{q}_h|^2(\boldsymbol{y}+\boldsymbol{t}(\boldsymbol{y})s)\,ds\,dS_{\boldsymbol{x}}\\ \lesssim & \int_e l(\boldsymbol{x})|(\boldsymbol{q}-\boldsymbol{q}_h)\cdot\boldsymbol{n}_\Gamma(\overline{\boldsymbol{x}})|^2\,dS_{\boldsymbol{x}} + \kappa^2\delta_e^2|||\boldsymbol{q}-\boldsymbol{q}_h|||_e^2\\ \lesssim & \,\delta_e\|\boldsymbol{q}-\boldsymbol{q}_h\|_{\Gamma_e}^2 + \kappa^2\delta_e^2|||\boldsymbol{q}-\boldsymbol{q}_h|||_e^2\end{aligned}$$

and from (4),

$$\kappa^2|||u-u_h|||_e^2 \lesssim \delta_e\|\boldsymbol{q}-\boldsymbol{q}_h\|_{\Gamma_e}^2 + \kappa^2\delta_e^2\|\boldsymbol{q}-\boldsymbol{q}_h\|_{K_{ext}^e}^2.$$

Then, by using (19), inverse inequality and (6), we obtain

$$\begin{aligned}\delta_e\|\boldsymbol{q}-\boldsymbol{q}_h\|_{\Gamma_e}^2 \leq & \, C_{\Gamma_e}\left(\|\boldsymbol{q}-\boldsymbol{q}_h\|_{K_{ext}^e}^2 + \delta_e\|\nabla(\boldsymbol{q}-\boldsymbol{q}_h)\|_{K_{ext}^e}^2\right)\\ \lesssim & \, C_{\Gamma_e}\left(\|\boldsymbol{q}-\boldsymbol{q}_h\|_{K_{ext}^e}^2 + \delta_e\left(\|\nabla\boldsymbol{I}^{\boldsymbol{q}}\|_{K_{ext}^e}^2 + h_e^{-2}(h_e^\perp)^{-1}\delta_e\|\boldsymbol{e}_h^{\boldsymbol{q}}\|_{K_e}^2\right)\right).\end{aligned}$$

Finally, by summing over $e \in \mathcal{E}_\Gamma$, using (42) and (16b), the result follows. □

6 Numerical results.

In this section we present two-dimensional numerical experiments to validate the theoretical orders of convergence of the approximations provided by the HDG method. We calculate the errors in the whole domain Ω, i.e., $e_u^\Omega := \|u-u_h\|_\Omega$ and $e_{\boldsymbol{q}}^\Omega := \|\boldsymbol{q}-\boldsymbol{q}_h\|_\Omega$; and also in the computational domain Ω_h, that is, $e_u^{\Omega_h} := \|u-u_h\|_{\Omega_h}$ and $e_{\boldsymbol{q}}^{\Omega_h} := \|\boldsymbol{q}-\boldsymbol{q}_h\|_{\Omega_h}$. Even more, we compute the projection error of the numerical trace, given by

$$e_h^{\widehat{u}} := \left(\sum_{K\in\Omega_h} h_K\|P_{M_h}u-\widehat{u}_h\|_{\partial K}\right)^{1/2}.$$

For each variable, we compute the experimental order of convergence

$$\text{e.o.c.} = -2\frac{\log\left(e_{\mathcal{T}_1}/e_{\mathcal{T}_2}\right)}{\log(N_{\mathcal{T}_1}/N_{\mathcal{T}_2})},$$

where $e_{\mathcal{T}_1}$ and $e_{\mathcal{T}_2}$ are the errors associated to the corresponding variable considering two consecutive meshes with $N_{\mathcal{T}_1}$ and $N_{\mathcal{T}_2}$ elements, respectively. In all the following numerical experiments we take the stabilization parameter $\tau = \kappa$.

6.1 Distance between Γ_h and Γ of order h^2.

We consider the domain Ω as the circle of radius 0.75 centered at the origin. By Remark 1 it is possible to construct a δ-admissible domain Ω_h whose boundary Γ_h is a piecewise linear interpolation of Γ with $\delta = \mathcal{O}(h^2)$ and $\alpha = 1/2$. Moreover, on each edge e of this $\delta-$admissible discretization of Ω_h, the vector $\boldsymbol{t}$ in (10f) is set to be the unit normal vector to e, see Remark 3.2 in [22].

Example 1. The source term and boundary condition are obtained through the exact solution $u(x,y)=\sin(x)\sin(y)$ and the stabilization parameter is taken as $\tau=\kappa$.

We display the history of convergence by considering $\kappa=1$ and $\kappa=100$ in Tables 1 and 2, respectively. When $\kappa=1$, the errors in $\boldsymbol{q}$ and u converge to zero with order $k+1$ as predicted by Corollary 16.1, since δ is of order h^2. Moreover, the numerical trace converge to the trace of u with order $k+2$ as we should expect. On the other hand, when $\kappa=100$, the errors reported in Table 2 shows a slightly better behavior than the one predicted by Corollary 16.1. We also infer that the errors in Ω_h^c are negligible compared to those of Ω.

k	N	$e_u^{\Omega_h}$	e.o.c.	e_u^{Ω}	e.o.c.	$e_{\boldsymbol{q}}^{\Omega_h}$	e.o.c.	$e_{\boldsymbol{q}}^{\Omega}$	e.o.c.	$e_h^{\widehat{u}}$	e.o.c.
1	234	2.45e−04	–	2.48e−04	–	6.31e−04	–	6.32e−04	–	1.99e−05	–
	485	1.29e−04	1.77	1.29e−04	1.78	3.10e−04	1.95	3.10e−04	1.96	7.31e−06	2.75
	918	6.46e−05	2.16	6.48e−05	2.17	1.56e−04	2.15	1.56e−04	2.15	2.54e−06	3.32
	1764	3.28e−05	2.07	3.29e−05	2.08	7.95e−05	2.07	7.95e−05	2.07	8.97e−07	3.19
	3546	1.68e−05	1.91	1.68e−05	1.92	4.05e−05	1.93	4.05e−05	1.93	3.23e−07	2.92
	7089	8.51e−06	1.97	8.51e−06	1.97	2.03e−05	2.00	2.03e−05	2.00	1.16e−07	2.96
	14291	4.24e−06	1.99	4.24e−06	1.99	1.01e−05	1.98	1.01e−05	1.98	4.07e−08	2.98
	28457	2.13e−06	2.00	2.13e−06	2.00	5.05e−06	2.02	5.05e−06	2.02	1.45e−08	3.00
2	234	5.64e−06	–	5.71e−06	–	1.31e−05	–	1.31e−05	–	1.90e−07	–
	485	1.92e−06	2.95	1.93e−06	2.97	4.70e−06	2.80	4.70e−06	2.81	4.48e−08	3.96
	918	7.10e−07	3.12	7.12e−07	3.13	1.66e−06	3.26	1.66e−06	3.26	1.23e−08	4.04
	1764	2.70e−07	2.97	2.70e−07	2.97	6.03e−07	3.10	6.03e−07	3.10	3.07e−09	4.26
	3546	9.73e−08	2.92	9.74e−08	2.92	2.19e−07	2.90	2.19e−07	2.90	7.84e−10	3.91
	7089	3.44e−08	3.00	3.45e−08	3.00	7.82e−08	2.97	7.82e−08	2.97	1.92e−10	4.06
	14291	1.22e−08	2.95	1.22e−08	2.95	2.78e−08	2.95	2.78e−08	2.95	4.42e−11	4.19
	28457	4.34e−09	3.01	4.34e−09	3.01	9.81e−09	3.02	9.81e−09	3.02	1.15e−11	3.91
3	234	1.30e−07	–	1.30e−07	–	1.52e−07	–	1.52e−07	–	4.13e−09	–
	485	3.45e−08	3.64	3.45e−08	3.64	3.81e−08	3.80	3.82e−08	3.80	6.77e−10	4.96
	918	8.51e−09	4.39	8.51e−09	4.39	9.63e−09	4.32	9.63e−09	4.32	1.33e−10	5.10
	1764	2.11e−09	4.27	2.11e−09	4.27	2.50e−09	4.13	2.50e−09	4.13	2.31e−11	5.36
	3546	5.60e−10	3.80	5.60e−10	3.81	6.63e−10	3.80	6.63e−10	3.80	4.17e−12	4.90
	7089	1.43e−10	3.94	1.43e−10	3.94	1.67e−10	3.98	1.67e−10	3.98	7.24e−13	5.06
	14291	3.59e−11	3.94	3.59e−11	3.94	4.25e−11	3.90	4.25e−11	3.90	1.13e−13	5.29
	28457	8.97e−12	4.03	8.97e−12	4.03	1.06e−11	4.03	1.06e−11	4.03	3.42e−14	3.48

Table 1: History of convergence of Example 1. Here, $\tau=\kappa$, $\kappa=1$ and $\delta=\mathcal{O}(h^2)$.

6.2 Distance between Γ_h and Γ of order h.

In practice, it is convenient to avoid the interpolation of the boundary Γ. Instead, it is preferable to consider a background where the domain Ω is *immersed*. Therefore, Ω_h is set as the union of the elements of the background mesh that are completely contained in Ω. In this case, the transferring paths can be constructed as in Section 2.4 in [11]. Unfortunately in this setting, Assumption (A.1) is not satisfied, since δ is of order h and we can not guarantee α to be equal to 1/2. However, we will see in the following two numerical experiments that the method still provides optimal approximations.

k	N	$e_u^{\Omega_h}$	e.o.c.	e_u^{Ω}	e.o.c.	$e_{\boldsymbol{q}}^{\Omega_h}$	e.o.c.	$e_{\boldsymbol{q}}^{\Omega}$	e.o.c.	$e_h^{\widehat{u}}$	e.o.c.
1	234	2.67e−04	–	2.67e−04	–	2.35e−02	–	2.35e−02	–	5.53e−04	–
	485	1.73e−04	1.19	1.73e−04	1.19	1.71e−02	0.88	1.71e−02	0.88	2.90e−04	1.77
	918	1.01e−04	1.70	1.01e−04	1.70	1.12e−02	1.33	1.12e−02	1.33	1.42e−04	2.25
	1764	5.53e−05	1.83	5.53e−05	1.84	6.72e−03	1.55	6.72e−03	1.55	6.69e−05	2.30
	3546	3.25e−05	1.52	3.25e−05	1.52	3.93e−03	1.54	3.93e−03	1.54	3.42e−05	1.92
	7089	1.72e−05	1.83	1.72e−05	1.83	2.17e−03	1.72	2.17e−03	1.72	1.70e−05	2.02
	14291	8.58e−06	1.99	8.58e−06	1.99	1.11e−03	1.90	1.11e−03	1.90	8.05e−06	2.13
	28457	3.40e−06	2.69	3.40e−06	2.69	5.08e−04	2.28	5.08e−04	2.28	3.02e−06	2.85
2	234	5.81e−06	–	5.82e−06	–	2.59e−04	–	2.61e−04	–	6.76e−06	–
	485	2.78e−06	2.02	2.78e−06	2.02	1.58e−04	1.35	1.59e−04	1.37	2.75e−06	2.46
	918	1.25e−06	2.51	1.25e−06	2.51	8.58e−05	1.91	8.60e−05	1.92	1.06e−06	2.98
	1764	4.95e−07	2.83	4.95e−07	2.84	4.04e−05	2.31	4.04e−05	2.31	4.22e−07	2.83
	3546	1.76e−07	2.96	1.76e−07	2.96	1.59e−05	2.68	1.59e−05	2.68	1.49e−07	2.99
	7089	4.86e−08	3.72	4.86e−08	3.72	4.52e−06	3.63	4.52e−06	3.63	3.74e−08	3.98
	14291	1.28e−08	3.81	1.28e−08	3.81	1.20e−06	3.77	1.20e−06	3.77	7.45e−09	4.60
	28457	3.70e−09	3.60	3.70e−09	3.60	3.51e−07	3.58	3.51e−07	3.58	1.14e−09	5.46
3	234	1.90e−07	–	1.90e−07	–	9.15e−06	–	9.18e−06	–	1.82e−07	–
	485	5.96e−08	3.18	5.96e−08	3.18	4.30e−06	2.07	4.30e−06	2.08	6.18e−08	2.97
	918	2.62e−08	2.58	2.62e−08	2.58	2.38e−06	1.86	2.38e−06	1.86	2.63e−08	2.68
	1764	5.89e−09	4.57	5.89e−09	4.57	5.71e−07	4.37	5.71e−07	4.37	5.36e−09	4.87
	3546	1.05e−09	4.94	1.05e−09	4.94	1.02e−07	4.92	1.02e−07	4.92	8.61e−10	5.24
	7089	1.63e−10	5.39	1.63e−10	5.39	1.55e−08	5.45	1.55e−08	5.45	7.74e−11	6.95
	14291	3.61e−11	4.29	3.61e−11	4.29	3.35e−09	4.37	3.35e−09	4.37	8.22e−12	6.40

Table 2: History of convergence of Example 1. Here, $\tau = \kappa$, $\kappa = 100$ and $\delta = \mathcal{O}(h^2)$.

Example 2. We consider the same domain and exact solution as in Example 1. In Table 3 are displayed the results for $\kappa = 1$ and can be observed that the error in all the variables is of order $k+1$. We emphasize that the last column for $k = 3$ is affected by round-off errors. On the other hand, for $\kappa = 100$, we also observe in Table 4 order of convergence of $k+1$ for all the variables when $k > 1$. When the polynomial degree of the approximation spaces is $k = 1$, the rate of convergence observed is less than 2, but it seems that will be approached by 2 for a sufficiently fine mesh.

Example 3. This example is motivated by the solution of a problem coming from modeling the scattering of an acoustic wave from a sound-soft impenetrable obstacle in a circular scatterer. We consider the annular domain $\Omega := \{(x, y) \in \mathbb{R}^2 : 0.5 < \sqrt{x^2+y^2} < 1\}$ and the truncated exact solution in polar coordinates with $M = 20$ and $\kappa = 7\pi$:

$$u(r,\theta) = -\frac{J_0(0.5\kappa)}{H_0^{(2)}(0.5\kappa)} H_0^{(2)}(r\kappa) - 2\sum_{m=1}^{M} i^m \frac{J_m(0.5\kappa)}{H_m^{(2)}(0.5\kappa)} H_m^{(2)}(r\kappa)\cos(m\theta),$$

where $\{J_m\}_m$ and $\{H_m^{(2)}\}_m$ denote the family of Bessel and Hankel functions, respectively. As usual, the source term and boundary condition are obtained from the solution. For a more wide explanation of the scattering problem see for example [12, 19]. The results in Table 5 show that the experimental

k	N	$e_u^{\Omega_h}$	e.o.c.	e_u^{Ω}	e.o.c.	$e_{\boldsymbol{q}}^{\Omega_h}$	e.o.c.	$e_{\boldsymbol{q}}^{\Omega}$	e.o.c.	$e_h^{\widehat{u}}$	e.o.c.
1	400	4.24e−04	–	5.54e−04	–	2.10e−03	–	3.01e−03	–	3.98e−04	–
	1680	1.81e−04	1.19	2.18e−04	1.30	8.77e−04	1.22	1.07e−03	1.44	1.75e−04	1.15
	7000	4.24e−05	2.03	4.66e−05	2.17	1.99e−04	2.08	2.42e−04	2.09	4.06e−05	2.05
	28504	9.73e−06	2.10	1.02e−05	2.17	4.48e−05	2.12	5.53e−05	2.10	9.23e−06	2.11
	115000	2.10e−06	2.20	2.14e−06	2.23	9.55e−06	2.22	1.24e−05	2.14	1.97e−06	2.22
	461656	5.07e−07	2.04	5.12e−07	2.06	2.30e−06	2.05	3.02e−06	2.03	4.73e−07	2.05
2	400	1.47e−05	–	2.10e−05	–	8.64e−05	–	1.19e−04	–	1.47e−05	–
	1680	3.22e−06	2.12	4.00e−06	2.31	1.64e−05	2.31	2.03e−05	2.47	3.21e−06	2.12
	7000	3.43e−07	3.14	3.83e−07	3.29	1.73e−06	3.15	2.15e−06	3.15	3.42e−07	3.14
	28504	3.68e−08	3.18	3.88e−08	3.26	1.87e−07	3.17	2.40e−07	3.13	3.66e−08	3.18
	115000	3.74e−09	3.28	3.84e−09	3.32	1.97e−08	3.23	2.69e−08	3.14	3.72e−09	3.28
	461656	4.51e−10	3.05	4.56e−10	3.06	2.39e−09	3.04	3.30e−09	3.02	4.48e−10	3.05
3	400	4.75e−07	–	6.21e−07	–	2.48e−06	–	3.70e−06	–	4.77e−07	–
	1680	8.35e−08	2.42	1.01e−07	2.53	4.12e−07	2.50	4.92e−07	2.81	8.36e−08	2.43
	7000	4.47e−09	4.10	4.92e−09	4.24	2.15e−08	4.14	2.49e−08	4.18	4.47e−09	4.10
	28504	2.30e−10	4.23	2.40e−10	4.30	1.09e−09	4.25	1.26e−09	4.25	2.29e−10	4.23
	115000	1.09e−11	4.38	1.11e−11	4.41	4.95e−11	4.43	6.07e−11	4.35	1.08e−11	4.38
	461656	4.60e−12	1.23	4.62e−12	1.26	5.11e−12	3.27	5.75e−12	3.39	4.60e−12	1.23

Table 3: History of convergence of Example 2. Here, $\tau = \kappa$, $\kappa = 1$ and $\delta = \mathcal{O}(h)$.

k	N	$e_u^{\Omega_h}$	e.o.c.	e_u^{Ω}	e.o.c.	$e_{\boldsymbol{q}}^{\Omega_h}$	e.o.c.	$e_{\boldsymbol{q}}^{\Omega}$	e.o.c.	$e_h^{\widehat{u}}$	e.o.c.
1	400	1.17e−04	–	1.73e−04	–	1.57e−02	–	1.69e−02	–	2.73e−04	–
	1680	2.43e−05	2.19	3.57e−05	2.20	5.18e−03	1.55	5.50e−03	1.56	4.54e−05	2.50
	7000	5.33e−06	2.12	6.35e−06	2.42	1.36e−03	1.87	1.40e−03	1.91	6.62e−06	2.70
	28504	1.93e−06	1.45	2.01e−06	1.64	3.71e−04	1.85	3.78e−04	1.87	1.84e−06	1.82
	115000	7.83e−07	1.29	7.89e−07	1.34	1.12e−04	1.72	1.13e−04	1.73	7.54e−07	1.28
	461656	2.51e−07	1.63	2.52e−07	1.64	3.21e−05	1.79	3.23e−05	1.80	2.45e−07	1.62
2	400	3.12e−06	–	6.48e−06	–	1.71e−04	–	2.71e−04	–	3.43e−06	–
	1680	5.16e−07	2.51	9.11e−07	2.73	4.68e−05	1.80	6.20e−05	2.05	4.87e−07	2.72
	7000	2.12e−07	1.25	2.23e−07	1.98	2.11e−05	1.12	2.16e−05	1.48	2.12e−07	1.17
	28504	4.39e−08	2.24	4.41e−08	2.31	4.37e−06	2.24	4.41e−06	2.27	4.38e−08	2.24
	115000	4.35e−09	3.31	4.36e−09	3.32	4.35e−07	3.31	4.38e−07	3.31	4.33e−09	3.32
	461656	4.59e−10	3.24	4.60e−10	3.24	4.60e−08	3.23	4.62e−08	3.23	4.57e−10	3.24
3	400	2.90e−08	–	1.72e−07	–	2.31e−06	–	7.82e−06	–	3.73e−08	–
	1680	1.48e−08	0.94	2.00e−08	3.00	1.46e−06	0.63	1.93e−06	1.95	1.49e−08	1.27
	7000	2.10e−09	2.73	2.17e−09	3.11	2.10e−07	2.72	2.17e−07	3.06	2.10e−09	2.75
	28504	1.02e−10	4.30	1.03e−10	4.34	1.02e−08	4.30	1.04e−08	4.33	1.02e−10	4.30
	115000	4.36e−12	4.53	4.37e−12	4.53	4.37e−10	4.52	4.42e−10	4.53	4.35e−12	4.53
	461656	2.66e−13	4.02	2.67e−13	4.03	2.67e−11	4.02	2.69e−11	4.03	2.66e−13	4.02

Table 4: History of convergence of Example 2. Here, $\tau = \kappa$, $\kappa = 100$ and $\delta = \mathcal{O}(h)$.

order of convergence is slightly less than $k+1$. Finally, in Figure 1 can be appreciated the magnitude of the approximation of the scalar variable obtained by the method.

k	N	$e_u^{\Omega_h}$	e.o.c.	e_u^{Ω}	e.o.c.	$e_{\boldsymbol{q}}^{\Omega_h}$	e.o.c.	$e_{\boldsymbol{q}}^{\Omega}$	e.o.c.	$e_{\widehat{u}}$	e.o.c.
1	520	2.88e-01	–	3.35e-01	–	6.40e+00	–	7.53e+00	–	2.75e-01	–
	2224	1.00e-01	1.45	1.11e-01	1.52	2.25e+00	1.44	2.54e+00	1.50	9.50e-02	1.46
	9280	2.51e-02	1.94	2.64e-02	2.00	5.70e-01	1.92	6.10e-01	1.99	2.37e-02	1.94
	37856	6.34e-03	1.96	6.52e-03	1.99	1.44e-01	1.95	1.51e-01	1.98	5.98e-03	1.96
	152784	1.70e-03	1.89	1.72e-03	1.91	3.84e-02	1.90	3.93e-02	1.93	1.61e-03	1.88
2	520	1.52e-01	–	1.92e-01	–	3.37e+00	–	3.94e+00	–	1.50e-01	–
	2224	3.36e-02	2.07	3.90e-02	2.19	7.48e-01	2.07	8.47e-01	2.12	3.35e-02	2.06
	9280	3.98e-03	2.99	4.27e-03	3.10	8.82e-02	2.99	9.51e-02	3.06	3.96e-03	2.99
	37856	5.11e-04	2.92	5.30e-04	2.97	1.14e-02	2.91	1.21e-02	2.94	5.09e-04	2.92
	152784	7.04e-05	2.84	7.16e-05	2.87	1.55e-03	2.85	1.60e-03	2.90	7.02e-05	2.84
3	520	9.97e-02	–	1.23e-01	–	2.23e+00	–	2.62e+00	–	9.97e-02	–
	2224	9.87e-03	3.18	1.14e-02	3.28	2.23e-01	3.16	2.59e-01	3.19	9.87e-03	3.18
	9280	5.34e-04	4.08	5.72e-04	4.18	1.22e-02	4.07	1.36e-02	4.12	5.34e-04	4.08
	37856	3.48e-05	3.89	3.61e-05	3.93	8.03e-04	3.87	8.75e-04	3.91	3.47e-05	3.89
	152784	2.34e-06	3.87	2.38e-06	3.90	5.37e-05	3.88	5.61e-05	3.94	2.34e-06	3.87

Table 5: History of convergence of Example 3. Here, $\tau=\kappa$, $\kappa=7\pi$ and $\delta=\mathcal{O}(h)$.

7 Concluding remarks and discussion.

We carried out a stability analysis based on a duality argument of the proposed unfitted HDG method for the mixed form of the Helmholtz equation defined in a non-polyhedral domain with first order boundary conditions. One of the novelties of our work is the introduction of a way to transfer a given Robin boundary data to the computational boundary of the unfitted domain. Moreover, the framework presented in this paper provides the tools to analyze the transference of Neumann data.

We performed an stability analysis making explicit the dependence on the wavenumber κ, the meshsize h and the gap δ between Ω and Ω_h, under certain closeness assumptions between Γ_h and Γ. This resutl was achieved by combining the known analyses of HDG schemes developed for problems posed in polyhedral domains with the boundary data transferring technique. In addition, the stability estimate was employed to deduce optimal convergence rates of the scheme. Numerical experiments were included to show the optimal performance of the numerical scheme, even in cases that are not completely covered by the theory, indicating the capability of the method to deal with problems defined in domains with complex geometries. In this direction, we plan to analyze the possibility of relaxing Assumption (A.1) in order to allow δ to be only of order h, according to what we have observed in the numerical simulations.

Another interesting approach to show stability without any constraint on the mesh can be obtained by employing a Rellich identity, in which the domain Ω is assumed to be star-shaped as it was considered by [13] in the polyhedral case. In the context of our unfitted HDG method, it is also possible to make use of a Rellich identity to avoid a meshsize restriction in most of the estimates. However, Assumption (A.1) still imposes a restriction on h and δ that depends on the wavenumber. In this sense, it is natural to expect that δ should be small enough for a high wavenumber since the

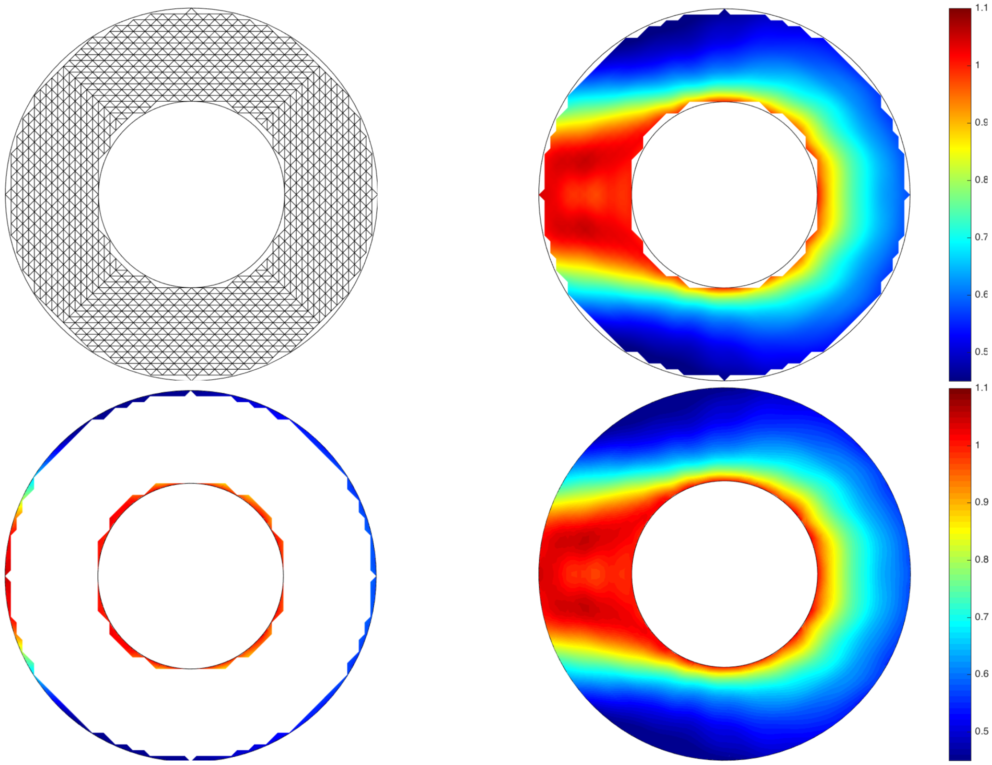

Figure 1: Example 3 with $k = 3$ and a mesh (top-left) with $N = 2224$. Approximation $|u_h|$ in the computational domain Ω_h (top-right), in the extrapolation region Ω_h^c (bottom-left) and in the physical domain Ω (bottom-right).

identity to transfer the boundary data depends linearly on κ (cf. (10f)). Once again, we believe this assumption could be relaxed at least on the dependence on h and this will be subject of future work.

Acknowledgements

M. Solano was partially funded by ANID–Chile projects through Fondecyt Nº1200569 and ACE 210010 and Centro de Modelamiento Matematico (FB210005). As a convention, the names of the authors are alphabetically order. All authors contributed equally in this article.

References

[1] I. M. Babuska and S. A. Sauter, *Is the pollution effect of the FEM avoidable for the Helmholtz equation considering high wave numbers?*, SIAM Journal on numerical analysis, 34 (1997), pp. 2392–2423.

[2] S. Brenner and R. Scott, *The mathematical theory of finite element methods*, vol. 15, Springer Science & Business Media, 2007.

[3] H. Chen, P. Lu, and X. Xu, *A hybridizable discontinuous Galerkin method for the Helmholtz equation with high wave number*, SIAM Journal on Numerical Analysis, 51 (2013), pp. 2166–2188.

[4] B. Cockburn, J. Gopalakrishnan, and R. D. Lazarov, *Unified hybridization of discontinuous Galerkin, mixed, and continuous Galerkin methods for second order elliptic problems*, SIAM J. Numer. Anal., 47 (2009), pp. 1319–1365.

[5] B. Cockburn, J. Gopalakrishnan, and F. Sayas, *A projection-based error analysis of HDG methods*, Math. Comp., 79 (2010), pp. 1351–1367.

[6] B. Cockburn, J. Gopalakrishnan, and F.-J. Sayas, *A projection-based error analysis of HDG methods*, Mathematics of Computation, 79 (2010), pp. 1351–1367.

[7] B. Cockburn, D. Gupta, and F. Reitich, *Boundary-conforming discontinuous Galerkin methods via extensions from subdomains*, Journal of Scientific Computing, 42 (2009), pp. 144–184.

[8] B. Cockburn, W. Qiu, and K. Shi, *Conditions for superconvergence of HDG methods for second-order elliptic problems*, Mathematics of Computation, 81 (2012), pp. 1327–1353.

[9] B. Cockburn, W. Qiu, and M. Solano, *A priori error analysis for HDG methods using extensions from subdomains to achieve boundary conformity*, Mathematics of computation, 83 (2014), pp. 665–699.

[10] B. Cockburn and F.-J. Sayas, *Divergence-conforming HDG methods for Stokes flows*, Math. Comp., 83 (2014), pp. 1571–1598.

[11] B. Cockburn and M. Solano, *Solving Dirichlet boundary-value problems on curved domains by extensions from subdomains*, SIAM Journal on Scientific Computing, 34 (2012), pp. A497–A519.

[12] D. Colton, *Partial Differential Equations: An Introductions*, The Random House, New York, 1988.

[13] J. Cui and W. Zhang, *An analysis of HDG methods for the Helmholtz equation*, IMA Journal of Numerical Analysis, 34 (2013), pp. 279–295.

[14] P. Cummings and X. Feng, *Sharp regularity coefficient estimates for complex-valued acoustic and elastic Helmholtz equations*, Mathematical Models and Methods in Applied Sciences, 16 (2006), pp. 139–160.

[15] J. Gopalakrishnan, M. Solano, and F. Vargas, *Dispersion analysis of HDG methods*, Journal of Scientific Computing, 77 (2018), pp. 1703–735.

[16] R. Griesmaier and P. Monk, *Error analysis for a hybridizable discontinuous Galerkin method for the Helmholtz equation*, Journal of Scientific Computing, 49 (2011), pp. 291–310.

[17] U. Hetmaniuk, *Stability estimates for a class of Helmholtz problems*, Communications in Mathematical Sciences, 5 (2007), pp. 635–636.

[18] T. Hughes, J. Cottrell, and Y. Bazilevs, *Isogeometric analysis: Cad, finite elements, nurbs, exact geometry and mesh refinement*, Computer Methods in Applied Mechanics and Engineering, 194 (2005), pp. 4135–4195.

[19] S. Kapita and P. Monk, *A plane wave discontinuous Galerkin method with a Dirichlet-to-Neumann boundary condition for the scattering problem in acoustics*, Journal of Computational and Applied Mathematics, 327 (2018), pp. 208–225.

[20] M. Lenoir, *Optimal isoparametric finite elements and error estimates for domains involving curved boundaries*, SIAM Journal on Numerical Analysis, 23 (1986), pp. 562–580.

[21] N.-C. Nguyen, J. Peraire, M. Solano, and S. Terrana, *An HDG method for non-matching meshes*, Preprint 2020-09, Centro de Investigación en Ingeniería Matemática (CI^2MA), Universidad de Concepción, Chile, (2020).

[22] R. Oyarzúa, M. Solano, and P. Zúñiga, *A high order mixed-FEM for diffusion problems on curved domains*, Journal of Scientific Computing, 79 (2019), pp. 49–78.

[23] R. Oyarzúa, M. Solano, and P. Zúñiga, *A priori and a posteriori error analyses of a high order unfitted mixed-FEM for Stokes flow*, Computer Methods in Applied Mechanics and Engineering, 360 (2020), p. 112780.

[24] C. S. Peskin, *Flow patterns around heart valves: A numerical method*, Journal of Computational Physics, 10 (1972), pp. 252–271.

[25] W. Qiu, M. Solano, and P. Vega, *A high order HDG method for curved-interface problems via approximations from straight triangulations*, Journal of Scientific Computing, 69 (2016), pp. 1384–1407.

[26] N. Sánchez, T. Sánchez-Vizuet, and M. E. Solano, *Error analysis of an unfitted HDG method for a class of non-linear elliptic problems*, arXiv preprint arXiv:2105.03560v1, (2021).

[27] N. Sánchez, T. Sánchez-Vizuet, and M. E. Solano, *A priori and a posteriori error analysis of an unfitted HDG method for semi-linear elliptic problems*, Numerische Mathematik, 148 (2021), pp. 919–958.

[28] T. Sánchez-Vizuet and M. Solano, *A Hybridizable discontinuous Galerkin solver for the Grad-Shafranov equation*, Computer Physics Communications, 235 (2019), pp. 120–132.

[29] T. Sánchez-Vizuet, M. E. Solano, and A. J. Cerfon, *Adaptive hybridizable discontinuous Galerkin discretization of the Grad–Shafranov equation by extension from polygonal subdomains*, Computer Physics Communications, 255 (2020), p. 107239.

[30] M. Solano and F. Vargas, *A high order HDG method for Stokes flow in curved domains*, Journal of Scientific Computing, 79 (2019), pp. 1550–1533.

[31] ——, *An unfitted HDG method for Oseen equations*, vol. 399, Elsevier, 2022.

[32] B. Zhu and H. Wu, *Hybridizable discontinuous Galerkin methods for Helmholtz equation with high wave number. part i: Linear case*, Preprint, (2020). (arXiv:2004.14553v1).

Centro de Investigación en Ingeniería Matemática (CI²MA)

PRE-PUBLICACIONES 2021

2021-16 Sergio Caucao, Gabriel N. Gatica, Juan P. Ortega: *A fully-mixed formulation in Banach spaces for the coupling of the steady Brinkman–Forchheimer and double-diffusion equations*

2021-17 David Mora, Alberth Silgado: *A C1 virtual element method for the stationary quasi-geostrophic equations of the ocean*

2021-18 Alfredo Bermúdez, Bibiana López-Rodríguez, Francisco José Pena, Rodolfo Rodríguez, Pilar Salgado, Pablo Venegas: *Numerical solution of an axisymmetric eddy current model with current and voltage excitations*

2021-19 Raimund Bürger, Sonia Valbuena, Carlos A. Vega: *A well-balanced and entropy stable scheme for a reduced blood flow model*

2021-20 Gabriel N. Gatica, Cristian Inzunza, Ricardo Ruiz-Baier, Felipe Sandoval: *A posteriori error analysis of Banach spaces-based fully-mixed finite element methods for Boussinesq-type models*

2021-21 David Mora, Iván Velásquez: *A* C^1–C^0 *conforming virtual element discretization for the transmission eigenvalue problem*

2021-22 Ricardo Oyarzúa, Manuel Solano, Paulo Zuñiga: *Analysis of an unfitted mixed finite element method for a class of quasi-Newtonian Stokes flow*

2021-23 Felisia A. Chiarello, Harold D. Contreras, Luis M. Villada: *Nonlocal reaction traffic flow model with on-off ramps*

2021-24 Sergio Caucao, Ricardo Oyarzúa, Segundo Villa-Fuentes, Ivan Yotov: *A three-field Banach spaces-based mixed formulation for the unsteady Brinkman-Forchheimer equations*

2021-25 Reinaldo Campos-Vargas, Esther Carrera, Bruno G. Defilippi, Claudia Fuentealba, Ignacia Hernández, Maarten Hertog, Claudio Meneses, Gerardo Nuñez, Diego Paredes, Romina Pedreschi, Virgilio Uarrota: *Transcriptome and hormone analyses reveals differences in physiological age of "Hass" avocado fruit*

2021-26 Tomás Barrios, Edwin Behrens, Rommel Bustinza: *Numerical analysis of a stabilized mixed method applied to incompressible elasticity problems with Dirichlet and with mixed boundary conditions*

2021-27 Liliana Camargo, Manuel Solano: *A high order unfitted HDG method for the Helmholtz equation with first order absorbing boundary condition*

Para obtener copias de las Pre-Publicaciones, escribir o llamar a: Director, Centro de Investigación en Ingeniería Matemática, Universidad de Concepción, Casilla 160-C, Concepción, Chile, Tel.: 41-2661324, o bien, visitar la página web del centro: `http://www.ci2ma.udec.cl`




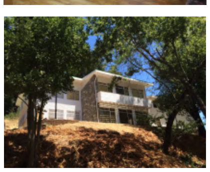

Centro de Investigación en
Ingeniería Matemática (CI^{2}MA)
Universidad de Concepción

Casilla 160-C, Concepción, Chile
Tel.: 56-41-2661324/2661554/2661316
http://www.ci2ma.udec.cl